

**Observation of Odderon Effects at LHC energies –
A Real Extended Bialas-Bzdak Model Study**

T. Csörgő

Wigner Research Centre for Physics

H-1525 Budapest 114, P.O.Box 49, Hungary

EKE KRC, H-3200 Gyöngyös, Mátrai út 36, Hungary

tcsorgo@cern.ch

I. Szanyi

Eötvös Loránd University,

H-1117 Budapest, Pázmány Péter s., 1/A Hungary

Wigner Research Centre for Physics

H-1525 Budapest 114, P.O.Box 49, Hungary

istvan.szanyi@cern.ch

Abstract

The unitarily extended Bialas-Bzdak model of elastic proton-proton scattering is applied, without modifications, to describe the differential cross-section of elastic proton-antiproton collisions in the TeV energy range, and to extrapolate these differential cross-sections to LHC energies. In this model-dependent study we find that the differential cross-sections of elastic proton-proton collision data at 2.76 and 7 TeV energies differ significantly from the differential cross-section of elastic proton antiproton collisions extrapolated to these energies. The difference is larger than the theoretical error on these extrapolations. On the other hand, the elastic proton-proton differential cross-sections, extrapolated to 1.96 TeV energy with the help of this extended Bialas-Bzdak model do not differ significantly from that of elastic proton-antiproton collisions at this particular energy, within the theoretical errors of the extrapolation. Taken together these results provide a model-dependent, but statistically significant evidence for a crossing-odd component of the elastic scattering amplitude. Obtained from the comparison of the extrapolated $p\bar{p}$ elastic differential cross-section to measured pp data at $\sqrt{s} = 2.76$ TeV, within this model and in the $0.372 \leq -t \leq 0.74$ range, the probability of Odderon observation is $P = 1 - CL \geq 0.99999999999891$, corresponding to a confidence level of $CL \leq 1.09 \times 10^{-12}$ and to an at least 7.1σ statistical significance. Compared to these values, the extrapolation of $p\bar{p}$ differential cross-section up to $\sqrt{s} = 7$ TeV results in an even larger model dependent significance and observation probability of Odderon effects.

I. INTRODUCTION

Recently the TOTEM experiment measured differential cross-sections of elastic proton-proton collisions in the TeV energy range, from $\sqrt{s} = 2.76$ through 7 and 8 to 13 TeV, together with the total, elastic and inelastic cross-sections and the real to imaginary ratio of the scattering amplitude at vanishing four-momentum transfer. These measurements provided surprises and unexpected results. First of all, the shape of the differential cross-section of elastic scattering at $\sqrt{s} = 7$ TeV was different from all the predictions.

The total cross-section increased with increasing \sqrt{s} according to theoretical expectations based on Pomeron-exchange, corresponding experimentally to the production of large rapidity gaps in high energy proton-proton and proton-antiproton collisions. These events correspond to large angular regions where no particle is produced. Their fraction, in particular the ratio of the elastic to the total proton-proton cross-section is increased above 25 % at LHC energies.

In the language of Quantum Chromo Dynamics (QCD), the field theory of strong interactions, Pomeron-exchange corresponds to the exchange of even number of gluons with vacuum quantum numbers. In 1973, a crossing-odd counterpart to the Pomeron was proposed by L. Lukaszuk and B. Nicolescu, the so-called Odderon [1]. In QCD, Odderon exchange corresponds to the t -channel exchange of a color-neutral gluonic compound state consisting of an odd number of gluons, as noted by Bartels, Vacca and Lipatov in 1999 [2].

The Odderon effects remained elusive for a long time, due to lack of a definitive and statistically significant experimental evidence for the Odderon effects.

A direct way to probe the Odderon in elastic scattering is by comparing the differential cross-section of particle-particle and particle-antiparticle scattering at sufficiently high energies [3, 4]. Such a search was published at the ISR energy of $\sqrt{s} = 53$ GeV in 1985 [5], that resulted in an indication of the Odderon, corresponding to a 3.35σ significance level obtained from a simple χ^2 calculation, based on 5 pp and 5 $p\bar{p}$ data points in the $1.1 \leq |t| \leq 1.5$ GeV² range (around the diffractive minimum). This significance is smaller than the 5σ threshold, traditionally accepted as a threshold for a discovery level observation in high energy physics. Furthermore, the analysis of ref. [5] did not utilize all the available data in the overlapping acceptance of the pp and $p\bar{p}$ measurements and did not include the overall (t -independent) relative normalization errors of the differential cross-sections. The colliding

energy of $\sqrt{s} = 53$ GeV was also not sufficiently large so the possible Reggeon exchange effects also were difficult to evaluate and control. These difficulties rendered the Odderon search at the ISR energies rather inconclusive, but nevertheless inspiring and indicative, motivating further studies.

In a series of recent papers, the TOTEM Collaboration published results with important implications for Odderon search. These papers studied elastic proton-proton collisions in the LHC energy range between $\sqrt{s} = 2.76$ and 13 TeV [6–9]. The total cross section, $\sigma_{\text{tot}}(s)$ was found to increase, while the real-to-imaginary ratio, $\rho(s)$, is found to decrease with increasing energy, first identified at $\sqrt{s} = 13$ TeV [6, 7]. These experimental results at vanishing four-momentum transfer were consistent with a possible Odderon effect and triggered an intense theoretical debate (see e.g. Refs. [10–27]). For example, Ref. [28] demonstrated that such an indication at $t = 0$ is not a unique Odderon signal, as such a behaviour can be attributed to secondary Reggeon effects. In spite of the rich experimental results and the hot theoretical debate, the Odderon remained rather elusive at vanishing four-momentum transfer even in the TeV energy range [29].

However, at larger four-momentum transfers, in the interference or diffractive minimum-maximum region, the Odderon signals are significant at LHC energies. Let us mention here only two of them here: the four-momentum transfer dependent nuclear slope parameter $B(t)$ and the scaling properties of elastic scattering at the TeV energy region.

Two independent, but nearly simultaneous phenomenological papers suggested that the four-momentum transfer dependence of the nuclear slope parameter, $B(t)$ is qualitatively different in elastic proton-proton and proton-antiproton collisions [12, 22]. The TOTEM experiment has demonstrated in ref. [9] that indeed in elastic pp collisions at $\sqrt{s} = 2.76$ TeV, the nuclear slope $B(t)$ is increasing (swings) before it decreases and changes sign in the interference (diffractive dip and bump or minimum-maximum) region. After the diffractive maximum, the nuclear slope becomes positive again. In contrast, elastic $p\bar{p}$ collisions measured by the D0 collaboration at the Tevatron energies of $\sqrt{s} = 1.96$ TeV did not show such a pronounced diffractive minimum-maximum structure, instead an exponentially decreasing cone region at low $-t$ with a constant $B(t)$ is followed by a shoulder structure, without a pronounced diffractive minimum and maximum structure. The TOTEM collaboration presented its results on the elastic pp differential cross-section at $\sqrt{s} = 2.76$ TeV and concluded in ref. [9] that “*under the condition that the effects due to the energy difference*

between TOTEM and D0 can be neglected, these results provide evidence for a colourless 3-gluon bound state exchange in the t -channel of the proton-proton elastic scattering”.

This energy gap has been closed recently, in a model-independent way, based on a re-analysis of already published data on the scaling properties of elastic scattering in both pp and $p\bar{p}$ collisions at TeV energies: Refs. [30–32] reported about a statistically significant Odderon signal in the comparison of the $H(x, s)$ scaling functions of elastic pp collisions at $\sqrt{s} = 7.0$ to that of $p\bar{p}$ collisions at $\sqrt{s} = 1.96$ TeV. The difference between these scaling functions carries an at least 6.26σ Odderon signal, if all the vertical and horizontal, point-to-point fluctuating and point-to-point correlated errors are taken into account. If the interpolation between the datapoints at 7 TeV is considered as a theoretical curve, the significance of the Odderon signal goes up to 6.55σ . Instead of comparing the cross sections directly, this method removes the dominant s dependent quantities, by scaling out the s -dependencies of $\sigma_{\text{tot}}(s)$, $\sigma_{\text{el}}(s)$, $B(s)$ and $\rho(s)$, as well as the normalization of the $H(x, s)$ scaling function, that also cancels the point-to-point correlated and t -independent normalization errors.

The model-independence of the results of refs. [12, 30–32] is an advantage when noting that the significant Odderon signal is seen in the comparison of the D0 and TOTEM data - in a model-independent way. However, a physical interpretation or a theoretical context is also desired, to gain a better understanding of the results, in order to have a more physical picture. To provide such a picture is one of the goals of our present manuscript. In this work, we continue a recent series of theoretical papers [33–36]. These studies investigated the differential cross-section of elastic pp collisions, but did not study the same effects in elastic $p\bar{p}$ collisions. The framework of these studies is the real extended and unitarized Bialas - Bzdak model, based on refs. [37–40]. This model considers protons as weakly bound states of valence quarks and diquarks, or $p = (q, d)$ for short. In a variation on this theme, the diquark in the proton may also be considered to be a weakly bound state of two valence quarks, leading to the $p = (q, (q, d))$ variant of the Bialas-Bzdak model [37, 38]. The model is based on Glauber’s multiple scattering theory of elastic collisions [41–43], assuming additionally, that all elementary distributions follow a random Gaussian elementary process, and can be characterized by the corresponding s -dependent Gaussian radii. These distributions include the parton or distribution inside the quark, characterized by a Gaussian radius $R_q(s)$, the distributions of the partons inside the diquarks, characterized by the Gaussian

radius $R_d(s)$ and the typical separation between the quarks and the diquarks characterized by the Gaussian radius $R_{qd}(s)$. In refs. [33, 34, 36] it was shown that the $p = (q, (q, q))$ variant of the Bialas-Bzdak model gives too many diffractive minima, while experimentally only a single diffractive minimum is observed in pp collisions. This is a result that is consistent with the earlier detailed studies of elastic nucleus-nucleus collisions in ref. [44], that observed that a single diffractive minimum occurs only in elastic deuteron - deuteron or $(p, n) + (p, n)$ collisions, so the number of diffractive minima increases as either of the elastically colliding composite objects develops a more complex internal structure.

In the original version of the Bialas-Bzdak model, the scattering amplitude was assumed to be completely imaginary [37]. This structure resulted in a completely vanishing differential cross-section at the diffractive minima. This model was supplemented by a real part, first perturbatively [33–35], subsequently in a non-perturbative and unitary manner [36]. This way a new parameter called $\alpha(s)$ was introduced, that controls the value of the differential cross-section at the diffractive minimum (it is not to be confused with the strong coupling constant of QCD, that we denote in this work as α_s^{QCD}). The structure of this ReBB model is thus very interesting as there are only four s -dependent physical parameters: R_q , R_d , R_{qd} and α . However three out of these four parameters is a geometrical parameter, characterizing the s dependence of parton distributions inside the protons. Hence, it is natural to assume, that these distributions are the same inside protons and anti-protons, while the opacity parameter α may be different in elastic pp and $p\bar{p}$ collisions.

In this manuscript, we thus extend the unitarily real extended Bialas-Bzdak model (abbreviated as ReBB model) from elastic pp to elastic $p\bar{p}$ collisions exactly in the same form, as was described in Ref. [36]. We fit exactly the same four physical parameters to describe the differential cross-section of elastic proton-proton (pp) scattering. Later we shall see that at the same energy, the geometrical parameters in pp and $p\bar{p}$ collisions are apparently consistent with one another, within the systematic errors of the analysis we obtain the same $R_q(s)$, $R_d(s)$ and $R_{qd}(s)$ functions.

In this manuscript, we thus can investigate also the following independent questions:

- Is the real extended Bialas-Bzdak model of ref. [36] able to describe not only elastic pp but also $p\bar{p}$ collisions?
- Is it possible to characterize the Odderon with only one physical parameter: the

difference of the opacity parameter $\alpha(s)$ in pp and in $p\bar{p}$ collisions: $\alpha^{pp}(s) \neq \alpha^{p\bar{p}}(s)$?

We shall see that the answer to both of these questions is a definitive yes.

The structure of the manuscript is as follows. In Section II we recapitulate the definition of the key physical quantities in elastic scattering and mention their main relations. In Section III we present the various error definitions and the evaluated χ^2 formulae of both pp and $p\bar{p}$ datasets. Subsequently, in Section III we detail the optimization method while in Section IV we summarize our fit results, that form the basis of the extrapolations to the not yet measured energies. These extrapolations are validated and cross-checked in Section V, using some additional published data, that were not utilized so far to establish the s -dependencies of the ReBB model parameters. As a next step for establishing the reliability of the s -dependence of the model parameters, we performed also the so called sanity tests in Section VI: we have cross-checked that the trend reproduces in a statistically acceptable manner each of the measurements also at those energies where the trends were established. After establishing that the excitation function of the ReBB model reproduces the measured data, we predict the experimentally not yet available large- t differential cross-section of pp collisions at $\sqrt{s} = 0.9, 4, 5$ and 8 TeV and we present the extrapolations of the pp differential cross-sections measured at the LHC energies of 2.96 and 7.0 TeV to the Tevatron energies of 1.8 and 1.96 TeV. Vice versa, we also extrapolate the $p\bar{p}$ differential cross-sections from the Tevatron energies of $\sqrt{s} = 1.8$ and 1.96 TeV to the LHC energies of 2.76 and 7.0 TeV in Section VII. These results are discussed in detail in Section VIII. These discussions include the estimation of the non-linear corrections with the help of data at $\sqrt{s} = 23.5$ GeV ISR energies. The extrapolations are possible only because the three geometrical parameters, R_q , R_d and R_{qd} follow the same trends in both pp and $p\bar{p}$ collisions, while the trend of the opacity parameter α is determined with the help of additional measurements of the real-to-imaginary ratio $\rho_0(s)$ both for the pp and for the $p\bar{p}$ cases. These connections are detailed and derived in A. Finally, we summarize and conclude.

II. FORMALISM

The elastic amplitude $T(s, t)$ (where s is the squared central mass energy, and t is the squared four-momentum transfer) is defined in Ref. [36] by Eq. (6), Eq. (9) and Eq. (29). The experimentally measurable physical quantities, *i.e.* the elastic differential cross section, the total, elastic and inelastic cross sections and the parameter ρ are defined, correspondingly, as:

$$\frac{d\sigma}{dt}(s, t) = \frac{1}{4\pi} |T(s, t)|^2, \quad (1)$$

$$\sigma_{tot}(s) = 2\text{Im}T(s, t = 0), \quad (2)$$

$$\sigma_{el}(s) = \int dt \frac{d\sigma}{dt}(s, t), \quad (3)$$

$$\sigma_{in}(s) = \sigma_{tot}(s) - \sigma_{el}(s) \quad (4)$$

and

$$\rho(s) = \frac{\text{Re}T(s, t = 0)}{\text{Im}T(s, t = 0)}. \quad (5)$$

The earlier results show that the ReBB model gives statistically acceptable, good quality fits with $\text{CL} \geq 0.1\%$ to the pp differential cross section data from the ISR energies up to the 7 TeV LHC energy [36], in the $-t \geq 0.377 \text{ GeV}^2$ kinematic region. Continuing that study, in this work we apply exactly the same formalism, without any change, to the description of the differential cross-sections of proton-antiproton ($p\bar{p}$) scattering. We thus do not recapitulate the details of the model, they are given in ref. [36]. When fitting the differential cross-section at a given colliding energy \sqrt{s} , we fit four physical parameters R_q , R_d , R_{qd} and α . We repeat these fits for both pp and $p\bar{p}$ collisions at various values of s and plot the resulting fit parameters as a function of $\ln(s/s_0)$ to see the emerging trends. As detailed in the subsequent sections, the scale parameters R_q , R_d and R_{qd} apparently follow the same, nearly linear trend as a function of $\ln(s/s_0)$, while the trend for the $\alpha(s)$ points seem to differ between pp and $p\bar{p}$ collisions.

This extension thus allows us to search for Odderon effects by comparing the pp and $p\bar{p}$ differential cross sections at same energies and squared momentum transfer. Any significant difference between the pp and $p\bar{p}$ processes at the same energy at the TeV scale provides

an evidence for the Odderon exchange. The term Odderon comes from the S-matrix theory based Regge theory where all the strongly interacting particles follow the so called Regge trajectories [45], see also refs. [46, 47]. In QCD, the Odderon corresponds to a colourless 3-gluon bound state [2, 48], or more generally colourless bound state of odd number of gluons with a negative charge parity, that has a significant contribution even at asymptotically large colliding energies at large four-momentum transfer [48].

III. FITTING METHOD

Compered to the earlier ReBB study [36], in order to more precisely estimate the significance of a possible Odderon effect, here I use a more advanced form of χ^2 definition which relies on a method developed by the PHENIX Collaboration and described in detail in Appendix A of Ref. [49]. This method is based on the diagonalization of the covariance matrix, if the experimental errors can be separated to the following types of uncertainties:

- Type A errors which are point-to-point fluctuating (uncorrelated) systematic and statistical errors;
- Type B errors which are point-to-point varying but correlated systematic uncertainties, for which the point-to-point correlation is 100 %;
- Type C systematic errors which are point-independent, overall systematic uncertainties, that scale all the data points up and down by exactly the same, point-to-point independent factor.

In what follows we index these errors with the index of the data point as well as with subscripts a , b and c , respectively.

In the course of the minimization of the ReBB model let us use the following χ^2 function:

$$\chi^2 = \left(\sum_{j=1}^M \left(\sum_{i=1}^{n_j} \frac{(d_{ij} + \epsilon_{bj}\tilde{\sigma}_{bij} + \epsilon_{cj}d_{ij}\sigma_{cj} - th_{ij})^2}{\tilde{\sigma}_{ij}^2} + \epsilon_{bj}^2 + \epsilon_{cj}^2 \right) + \left(\frac{d_{\sigma_{tot}} - th_{\sigma_{tot}}}{\delta\sigma_{tot}} \right)^2 + \left(\frac{d_{\rho_0} - th_{\rho_0}}{\delta\rho_0} \right)^2 \right). \quad (6)$$

This definition includes type A, point-to-point uncorrelated errors, type B point-to-point dependent but correlated errors and type C, point independent correlated errors. Furthermore, not only vertical, but the frequently neglected horizontal errors are included too. Let us detail below the notation of this χ^2 definition, step by step:

- M is the number sub-datasets, corresponding to several, separately measured ranges of t , indexed with subscript j , at a given energy \sqrt{s} . Thus $\sum_{j=1}^M n_j$ gives the number of fitted data points at a given center of mass energy \sqrt{s} ;

- d_{ij} is the i th measured differential cross section data point in sub-dataset j and th_{ij} is the corresponding theoretical value calculated from the ReBB model;
- $\tilde{\sigma}_{ij}$ is the type A, point-to-point fluctuating uncertainty of the data point i in sub-dataset j , scaled by a multiplicative factor such that the fractional uncertainty is unchanged under multiplication by a point-to-point varying factor:

$$\tilde{\sigma}_{ij}^2 = \tilde{\sigma}_{aij} \left(\frac{d_{ij} + \epsilon_{bj}\tilde{\sigma}_{bij} + \epsilon_{cj}d_{ij}\sigma_{cj}}{d_{ij}} \right) \quad (7)$$

where the terms

$$\tilde{\sigma}_{kij} = \sqrt{\sigma_{kij}^2 + (d'_{ij}\delta_k t_{ij})^2}, \quad k \in \{a, b\}, \quad (8)$$

include also the A and B type horizontal errors on t following the propagation of the horizontal error to the χ^2 as utilized by the so-called effective variance method of the CERN data analysis programme ROOT; d'_{ij} denotes the numerical derivative in point t_{ij} with errors of type $k \in \{a, b\}$, denoted as $\delta_k t_{ij}$. The numerical derivative is calculated as

$$d'(t_{ij}) = \frac{d_{(i+1)j} - d_{ij}}{t_{(i+1)j} - t_{ij}}; \quad (9)$$

- The correlation coefficients for type B and C errors are denoted by ϵ_b and ϵ_c , respectively. These numbers are free parameters to fitted to the data, their best values are typically in the interval $(-1, 1)$.;
- The last two terms in Eq. (6) are to fit also the measured total cross-section and ratio ρ_0 values along the differential cross section data points; $d_{\sigma_{\text{tot}}}$ and d_{ρ_0} denote the measured total cross section and ratio ρ_0 values, $\delta\sigma_{\text{tot}}$ and $\delta\rho_0$ are their full errors, $\sigma_{\text{tot,th}}$ and $\rho_{0,\text{th}}$ are their theoretical value calculated from the ReBB model;

This scheme has been validated by evaluating the χ^2 from a full covariance matrix fit and from the PHENIX method of diagonalizing the covariance matrix of the differential cross-section of elastic pp scattering measured by TOTEM at $\sqrt{s} = 13$ TeV [6], using the Lévy expansion method of Ref. [12]. The fit with the full covariance matrix results the same minimum within one standard deviation of the fit parameters [32], hence in the same significance, as the fit with the PHENIX method. Based on this validation, we apply the PHENIX method in the data analysis described in this manuscript.

Let us not also, that in case of the $\sqrt{s} = 7$ TeV TOTEM data set, analysed below, the B type systematic errors, that shift all the data points together up or down with a t -dependent value are measured to be asymmetric [50]. This effect is handled by using the up or down type B errors depending on the sign of the correlation coefficient ϵ_b : for positive or negative sign of ϵ_b , we utilized the type B errors upwards, or downwards, respectively. Note that the type A errors, that enter the numerator of the χ^2 definition of eq. 6, are symmetric even in the case of this $\sqrt{s} = 7$ TeV pp dataset, so the χ^2 distribution can still be used to estimate the significances and confidence levels of the best fits even in this case.

IV. FIT RESULTS

The ReBB model was fitted to the proton-proton differential cross section data measured by the TOTEM Collaboration at $\sqrt{s} = 2.76, 7.0$ and 13 TeV, based on refs. [6, 9, 50] as well as to differential cross section data of elastic proton-antiproton scattering measured at $\sqrt{s} = 0.546$ and 1.96 TeV in refs. [51–53], respectively.

Similarly to earlier studies of refs. [34–37, 40], the model parameters $A_{qq} = 1$ and $\lambda = \frac{1}{2}$ were kept at constant values throughout the fitting procedure. Here A_{qq} corresponds to a normalization constant and λ describes the mass ratio of constituent quarks to diquarks in the $p = (q, d)$ version of the real extended Bialas-Bzak model of ref. [36]. Thus the number of free parameters of this model is reduced to four: R_{qd}, R_q, R_d and α . All of these four physical fit parameters may depend on the energy of the collision in the center of mass system, \sqrt{s} . Three out of the four physical parameters, $R_q(s), R_d(s)$ and $R_{qd}(s)$ are geometrical scale parameters, corresponding to the Gaussian radii that characterize the parton distribution inside the quarks as well as the diquarks, and the Gaussian distribution of the separation between the centers of the constituent quark and diquark, respectively. The last physical parameter $\alpha(s)$ is a kind of opacity parameter, that measures the strength of the real part of the scattering amplitude and is responsible for filling up the dip region of the differential cross-section. So it is natural to expect, that this $\alpha(s)$ parameter may carry an Odderon signal as its excitation function might be very different in elastic pp collisions, that feature a pronounced dip at every measured energy even in the TeV energy range [9], while in elastic $p\bar{p}$ collisions, a significant dip is lacking even in measurements in the TeV energy range [53]. It is also natural to expect that $R_q(s), R_d(s)$ and $R_{qd}(s)$ is the same function for pp and $p\bar{p}$ collisions, as the distribution of partons inside protons at a given energy is expected to be the same as that inside anti-protons, due to C symmetry. In this section, this is however not assumed but tested and the parameters of the ReBB model are determined at four different colliding energies in the TeV region, using pp data sets at $\sqrt{s} = 2.76$ and 7 TeV, and $p\bar{p}$ datasets at $\sqrt{s} = 0.546$ and 1.96 TeV. These fits were performed in the diffractive interference or dip and bump region, with datapoints before the diffractive minimum and after the maximum as well, in each case a the limited range not greater than $0.372 \leq -t \leq 1.2$ GeV². In this kinematic range, where the ReBB model provided a data description with a statistically acceptable fit quality, with confidence levels

CL ≥ 0.1 % in each case. Other data sets, that do not have sufficient amount of data in this interference region were utilized for cross-checks only, to test the extracted energy dependence of the model parameters.

In this manuscript, our aim is to extapolate the differential cross-section of elastic pp and $p\bar{p}$ collisions to exactly the same energies, in order to conclude in a model dependent way about the significance of an Odderon component in these data.

For this purpose, a model that can be used to study the excitation function of the pp and $p\bar{p}$ differential cross-sections in the $0.5 \leq \sqrt{s} \leq 8$ TeV domain is sufficient. The results of such kind of statistically acceptable quality fits are summarized in Table I and detailed below. Additionally, we also describe the current status of our fits to describe the differential cross-sections at $\sqrt{s} = 13$ TeV at the end of this section.

We thus describe three fits to pp differential cross section data sets at $\sqrt{s} = 2.76, 7$ and 13 TeV as well as two fits to $p\bar{p}$ differential cross section datasets at $\sqrt{s} = 0.546$ and 1.96 TeV, respectively. Experimental information on the type B, t -dependent correlated systematic errors is not publicly available for these fits. Our fit results are shown in Figs. 1-5. The fit range in the squared momentum transfer is chosen to be $0.37 \leq -t \leq 1.2$ GeV². The minimization of the χ^2 defined by Eq. (6) was done with Minuit and the parameter errors were estimated by using the MINOS algorithm which takes into account both parameter correlations and non-linearities. We accept the fit as a successful representation of the fitted data under the condition that the fit status is converged, the error matrix is accurate and the confidence level of the fit, CL is ≥ 0.1 %, as indicated on Figs. 1-4. As these criteria are not satisfied on Fig. 5, the parameters of this fit were not taken into account when determining the excitation functions or the energy dependence of the physical fit parameters in the few TeV energy range.

Let us now discuss each fit with in a bit more detail.

The $Spp\bar{S}$ differential cross section data on elastic $p\bar{p}$ collisions [51, 52] were measured in the squared momentum transfer range of $0.03 \leq |t| \leq 1.53$ GeV² which in the fitted range has been subdivided into two sub-ranges with different normalization uncertainties (type C errors): for $0.37 \leq |t| \leq 0.495$ GeV² $\sigma_c = 0.03$ and for $0.46 \leq |t| \leq 1.2$ GeV² $\sigma_c = 0.1$. In case of this data set, the vertical type A errors σ_{ai} are available but the horizontal type A errors ($\delta_a t_i$) and the type B errors either vertical (σ_{bi}) or horizontal ($\delta_b t_i$) were not published. The measured total cross section with its total uncertainty is $\sigma_{\text{tot}} = 61.26 \pm 0.93$ mb [54] while

ρ_0 value was measured at the slightly different energy of $\sqrt{s} = 0.541$ GeV. The total, elastic and inelastic cross sections and the parameter ρ are calculated according to Eqs. (2)-(5). The fit is summarized in Fig. 1. The fit quality is satisfactory, CL = 8.74 %. Compared to the available data in the literature[54] ($\sigma_{in} = 48.39 \pm 1.01$ mb, $\sigma_{el} = 12.87 \pm 0.3$ mb and $\rho = 0.135 \pm 0.015$ (measured at 541 GeV)) the model reproduces the experimental values of the forward measurables within one σ , thus these fit parameters represent the data in a statistically acceptable manner.

The elastic $p\bar{p}$ differential cross section data is available at $\sqrt{s} = 1.96$ TeV in the range of $0.26 \leq |t| \leq 1.20$ GeV², as published by the D0 Collaboration in ref. [53], with a type C normalization uncertainty of $\sigma_c = 0.144$. For this data set, the vertical type A and type B errors were not published separately. Actually, the quadratically added statistical and systematic uncertainties were published, and as the statistical errors are point to-point fluctuating, type A errors, in our analysis the combined t dependent D0 errors were handled as type A, combined statistical and systematic errors. Horizontal type A and type B errors were not published in ref. [53]. At this energy, we did not find published experimental σ_{tot} and ρ values. The values of the total cross section and parameter ρ at this energy, that we utilized in the fitting procedure, are the predicted values from the COMPETE Collaboration [55]: $\sigma_{tot} = 78.27 \pm 1.93$ mb and $\rho = 0.145 \pm 0.006$. The fit quality of the corresponding Fig. 2 is satisfactory, CL = 51.12 %, and the COMPETE values of forward measurables are reproduced within one standard deviation. We conclude that the corresponding ReBB model parameters represent the data in a statistically acceptable manner.

Based on the successful description of these two $p\bar{p}$ datasets at $\sqrt{s} = 0.546$ and 1.96 TeV, we find that the form of the ReBB model as specified for pp collisions in ref. [36] is able, without any modifications, to describe the differential cross-section of elastic $p\bar{p}$ collisions in the TeV energy range. Let us now discuss the new fits of the same model to elastic pp collisions in the TeV energy range.

At $\sqrt{s} = 2.76$ TeV, the differential cross section data of elastic pp collisions was measured in the t range of $0.072 \leq -t \leq 0.74$ GeV² by the TOTEM Collaboration [9]. Actually, this measurement was performed in two subranges: $0.072 \leq |t| \leq 0.462$ GeV² and $0.372 \leq |t| \leq 0.74$ GeV². Both ranges had the same normalization uncertainty of $\sigma_c = 0.06$. During the fit the t -dependent vertical statistical (type A) and vertical systematic (type B) errors, the normalization (type C) errors and the experimental value of the total cross section with its

total uncertainty ($\sigma_{\text{tot}} = 84.7 \pm 3.3$ mb [6]) were taken into account. Horizontal type A and type B errors are not published at this energy. The fit quality of the ReBB model is demonstrated on Fig. 3: the fit is satisfactory, with CL = 36.52 %. The experimental values of the forward measurables ($\sigma_{in} = 62.8 \pm 2.9$ mb, $\sigma_{el} = 21.8 \pm 1.4$ mb [6, 56]) are reproduced within one standard deviations. Experimental data is not yet available for parameter ρ , however the ReBB model value for ρ , calculated from the fitted ReBB model, is within the total error band of the COMPETE prediction [55]. We thus conclude that the corresponding ReBB model parameters represent the pp data at $\sqrt{s} = 2.76$ TeV in a statistically acceptable manner.

At $\sqrt{s} = 7$ TeV, the pp differential cross section data was published by the TOTEM Collaboration [50], measured in the range of $0.005 \leq |t| \leq 2.443$ GeV². The measurement was performed in two subranges: $0.005 \leq |t| \leq 0.371$ GeV² and $0.377 \leq |t| \leq 2.443$ GeV². Both ranges had the same normalization uncertainty of $\sigma_c = 0.042$. The fit includes only the second subrange with the t -dependent (both vertical and horizontal) statistical (type A) and systematic (type B) errors, the normalization (type C) error and the experimental values of the total cross section and the parameter ρ with their total uncertainties ($\sigma_{\text{tot}} = 98.0 \pm 2.5$ mb and $\rho = 0.145 \pm 0.091$ [57]). The fit quality of the corresponding Fig. 4) is statistically acceptable. with a CL = 0.95 %. The experimental values of the the forward measurables ($\sigma_{in} = 72.9 \pm 1.5$ mb, $\sigma_{el} = 25.1 \pm 1.1$ mb [57]) are reproduced by the fitted ReBB model within one sigma. We thus conclude that the corresponding ReBB model parameters represent these pp data at $\sqrt{s} = 7.0$ TeV in a statistically acceptable manner, in the fitted range of $0.005 \leq |t| \leq 2.443$ GeV², before and after the diffractive minimum.

At $\sqrt{s} = 8$ TeV, the TOTEM collaboration did not yet publish the final differential cross-section results in the range of the diffractive minimum and maximum. However, preliminary results were presented at conferences [58], and the differential cross-section in the low $-t$ was published in ref. [59]. We thus use this dataset for a cross-check only, but the lack of the data in the diffractive minimum prevents us to do a full ReBB model fit. Additional data at very low t , in the Coulomb-Nuclear Interference region is also available from TOTEM at this particular energy [60], however, in the present study we do not discuss the kinematic range, where Coulomb effects may play any role.

At $\sqrt{s} = 13$ TeV, the differential cross section data was measured by the TOTEM collaboration in the range of $0.03 \leq |t| \leq 3.8$ GeV² [8] with a normalization (type C)

uncertainty of $\sigma_c = 0.055$. As far as we know, the only statistically acceptable quality fit with $\text{CL} \geq 0.1\%$ to this dataset so far was obtained by some of us with the help of the model-independent Lévy series in ref. [12]. We also note that several new features show up in the soft observables of elastic scattering, with a threshold behaviour around $\sqrt{s} = 5 - 7$ TeV, certainly below 13 TeV [61].

We have cross-checked, if the ReBB model, that works reasonably well from $\sqrt{s} = 23.5$ GeV to 7 TeV, is capable to describe this data set in statistically acceptable manner, or not? The result was negative, as indicated on Fig. 5. This fit includes the t-dependent the statistical (type A) and systematic (type B) errors, the normalization (type C) error and the experimental values of the total cross section and the parameter ρ with their total uncertainties ($\sigma_{\text{tot}} = 110.5 \pm 2.4$ mb and $\rho = 0.09 \pm 0.01$ [7]). Neither the quality of the obtained fit, nor the description of the experimental values of the forward measurables like σ_{in} , σ_{el} or ρ turned out to be satisfactory, as $\text{CL} = 3.17 \times 10^{-11}\%$ only, and the published values of $\sigma_{\text{in}} = 79.5 \pm 1.8$ mb, $\sigma_{\text{el}} = 31.0 \pm 1.7$ mb [6]) were not reproduced by the fitted ReBB model within one standard deviation at this energy of $\sqrt{s} = 13$ TeV. However, the value of ρ was described surprisingly well. This TOTEM dataset is very detailed and precise and changes of certain trends in $B(s)$ and the ratio $\sigma_{\text{el}}(s)/\sigma_{\text{tot}}(s)$ are seen experimentally [61]. Theoretically, a new domain of hollowness or a black ring-like structure is seen in the model-independent analysis of the shadow profile at these energies, using the technique of Lévy series [12]. We conclude that the ReBB model needs to be generalized to have a stronger non-exponential feature at low $-t$ to accommodate the new features of the differential cross-section data at $\sqrt{s} = 13$ TeV or larger energies. This work is currently in progress, but goes well beyond the scope of the current manuscript. Most importantly, such a generalization is not necessary for a comparison of the differential cross-sections of elastic pp and $p\bar{p}$ collisions in the few TeV range, as we have to bridge only a logarithmically small energy difference between the top D0 energy of $\sqrt{s} = 1.96$ TeV and the lowest TOTEM energy of $\sqrt{s} = 2.76$ TeV.

We thus find, that the Real Extended Bialas - Bzdak model describes effectively and in a statistically acceptable manner the differential cross-sections of elastic pp and $p\bar{p}$ collisions in the few TeV range of $0.546 \leq \sqrt{s} \leq 7$ TeV. Its physical fit parameters represent the data and their energy dependence thus can be utilized to determine the excitation function of these model parameters. The values of the physical fit parameters and their errors obtained from

the above discussed physically and statistically acceptable fits are summarized in Table I.

We thus conclude, that this Real Extended Bialas-Bzdak model is good enough to extrapolate the differential cross-section of elastic pp collisions down to $\sqrt{s} = 0.546$ and 1.96 TeV, and to extrapolate the same of elastic $p\bar{p}$ collisions up to $\sqrt{s} = 2.76$ and 7 TeV. We duly note that, in order to evaluate similar observables at $\sqrt{s} = 13$ TeV or at even higher energies in a realistic manner, this model needs to be generalized and further developed.

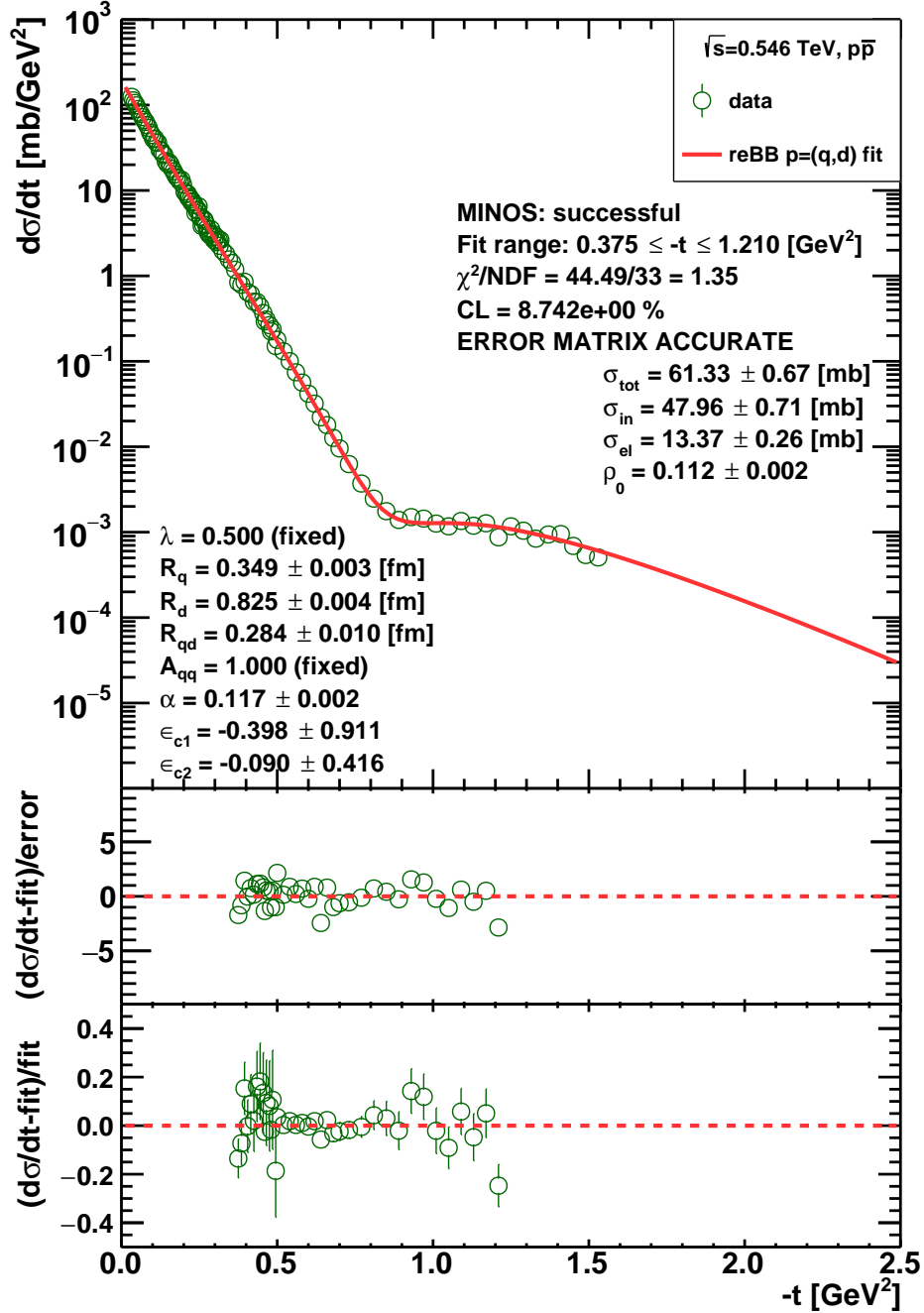


FIG. 1. The fit of the ReBB model to the $p\bar{p}$ SPS $\sqrt{s} = 0.546$ TeV data [51, 52] in the range of $0.37 \leq -t \leq 1.2$ GeV². The fit includes the published errors, that are statistical (type A) and the normalization (type C) uncertainties, as well as the experimental value of the total cross section with its full error according to Eq. (6). The fitted parameters are shown in the left bottom corner and their values are rounded up to three decimal digits. The fit quality parameters and the values of the total, inelastic and elastic cross-sections as well as the value of the ρ parameter are summarized in the top right part of the plot.

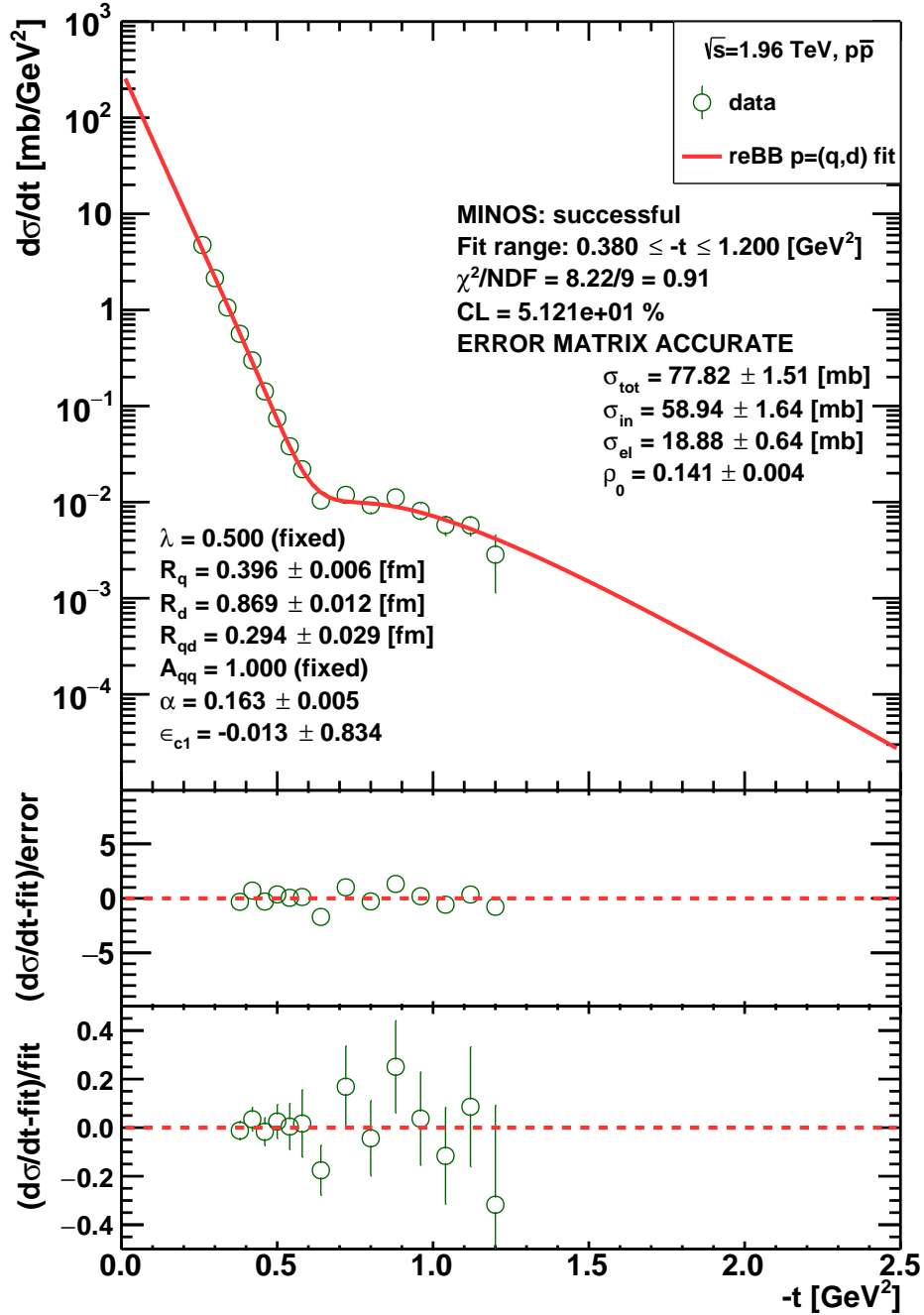


FIG. 2. The fit of the ReBB model to the $p\bar{p}$ D0 $\sqrt{s} = 1.96 \text{ TeV}$ data [53] in the range of $0.37 \leq -t \leq 1.2 \text{ GeV}^2$. The fit includes the t -dependent statistical and systematic uncertainties added together quadratically and treated as type A errors as well as the normalization (type C) uncertainty according to Eq. (6). The values of the total cross section and parameter ρ used in the fit are the predicted values from the COMPETE Collaboration [55]. Otherwise, same as Fig. 1.

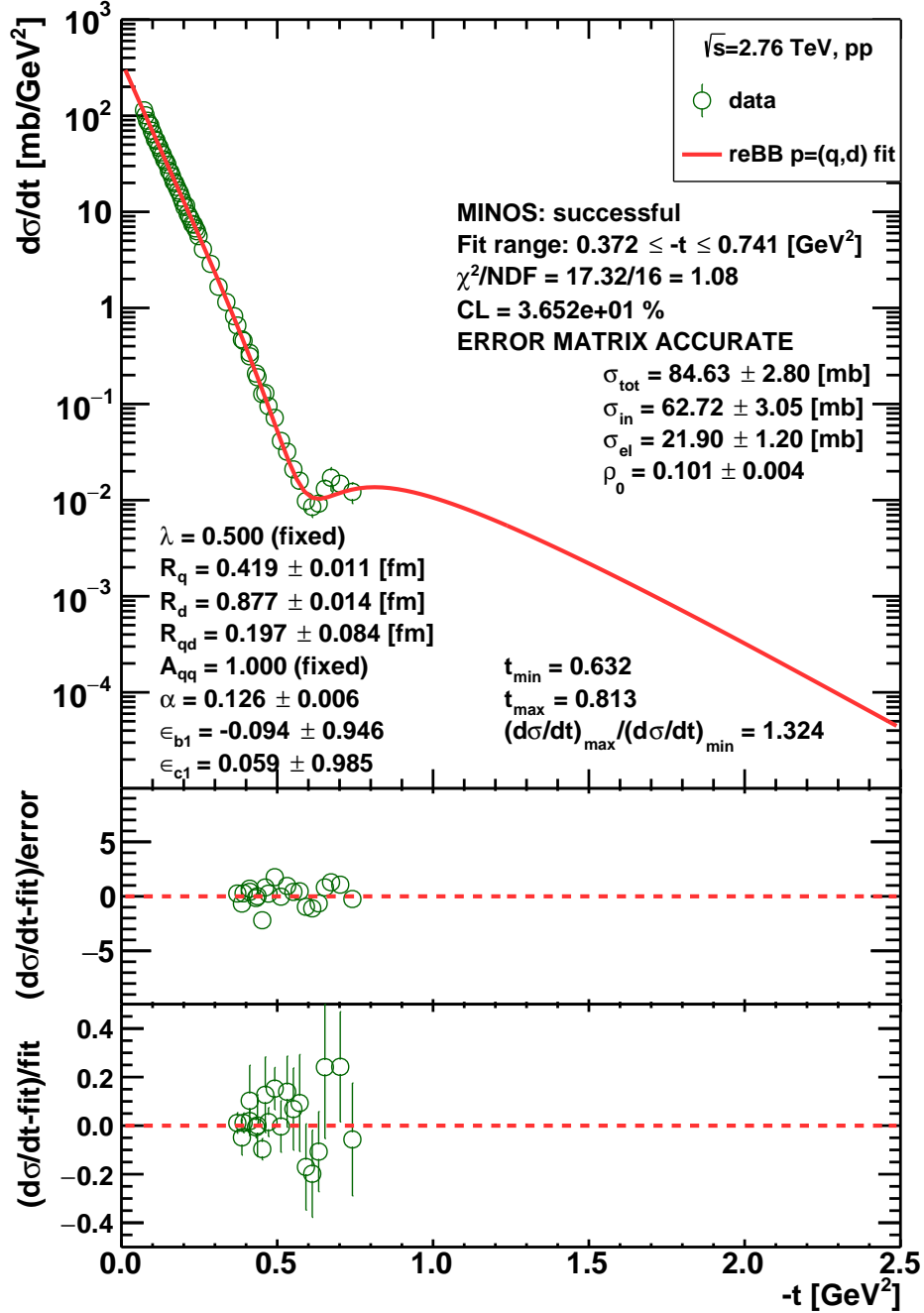


FIG. 3. The fit of the ReBB model to the pp TOTEM $\sqrt{s} = 2.76$ TeV data in the range of $0.37 \leq -t \leq 0.74$ GeV² [9]. The fit includes the t -dependent statistical (type A) and systematic (type B) uncertainties, the normalization (type C) uncertainty and the experimental value of the total cross section with its full error according to Eq. (6). Otherwise, same as Fig. 1.

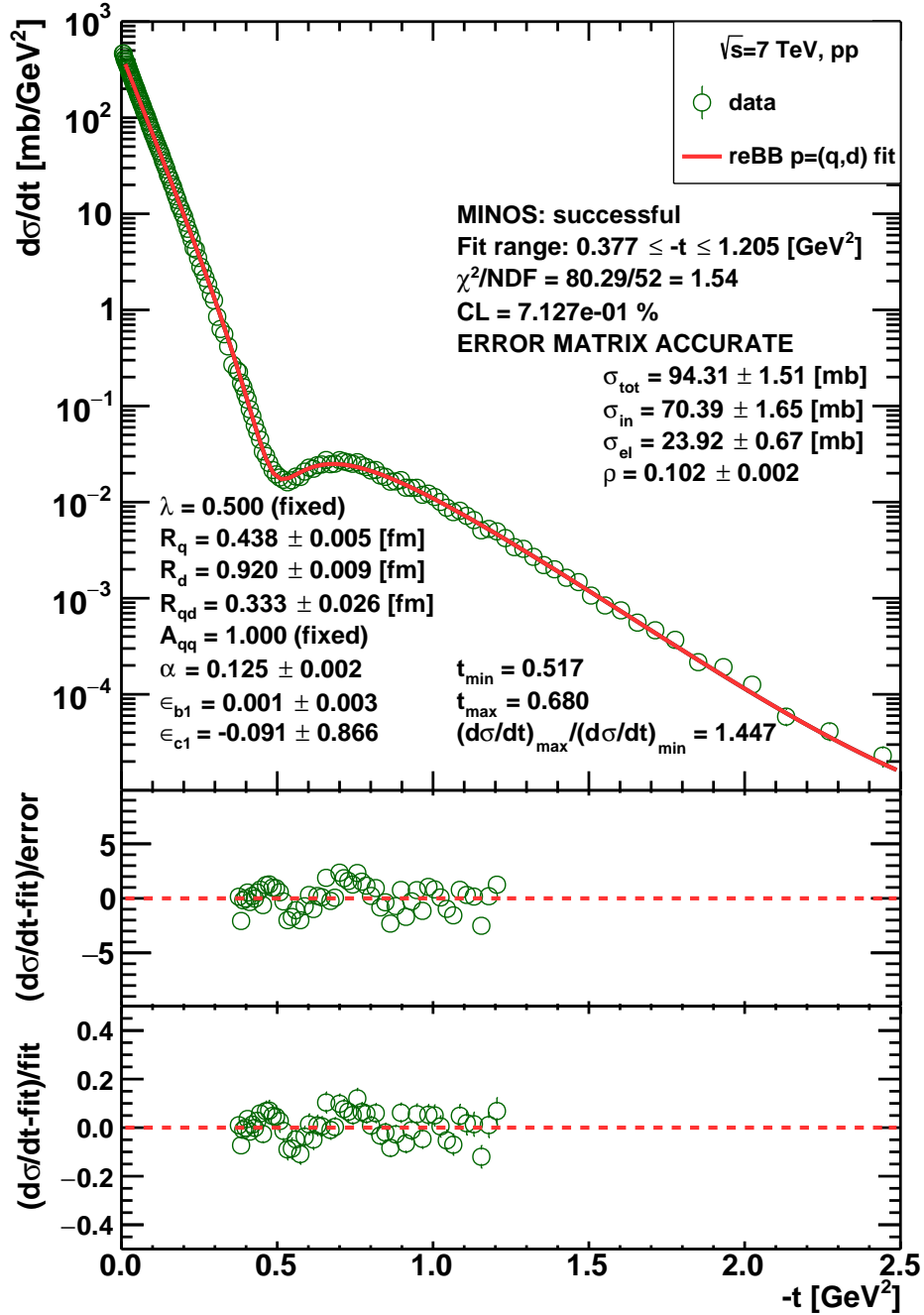


FIG. 4. The fit of the ReBB model to the pp TOTEM $\sqrt{s} = 7$ TeV data in the range of $0.37 \leq -t \leq 1.2$ GeV² [50]. The fit includes the t -dependent statistical (type A) and systematic (type B) uncertainties, the normalization (type C) uncertainty and the experimental values of the total cross section and parameter ρ with their full error according to Eq. (6). Otherwise, same as Fig. 1.

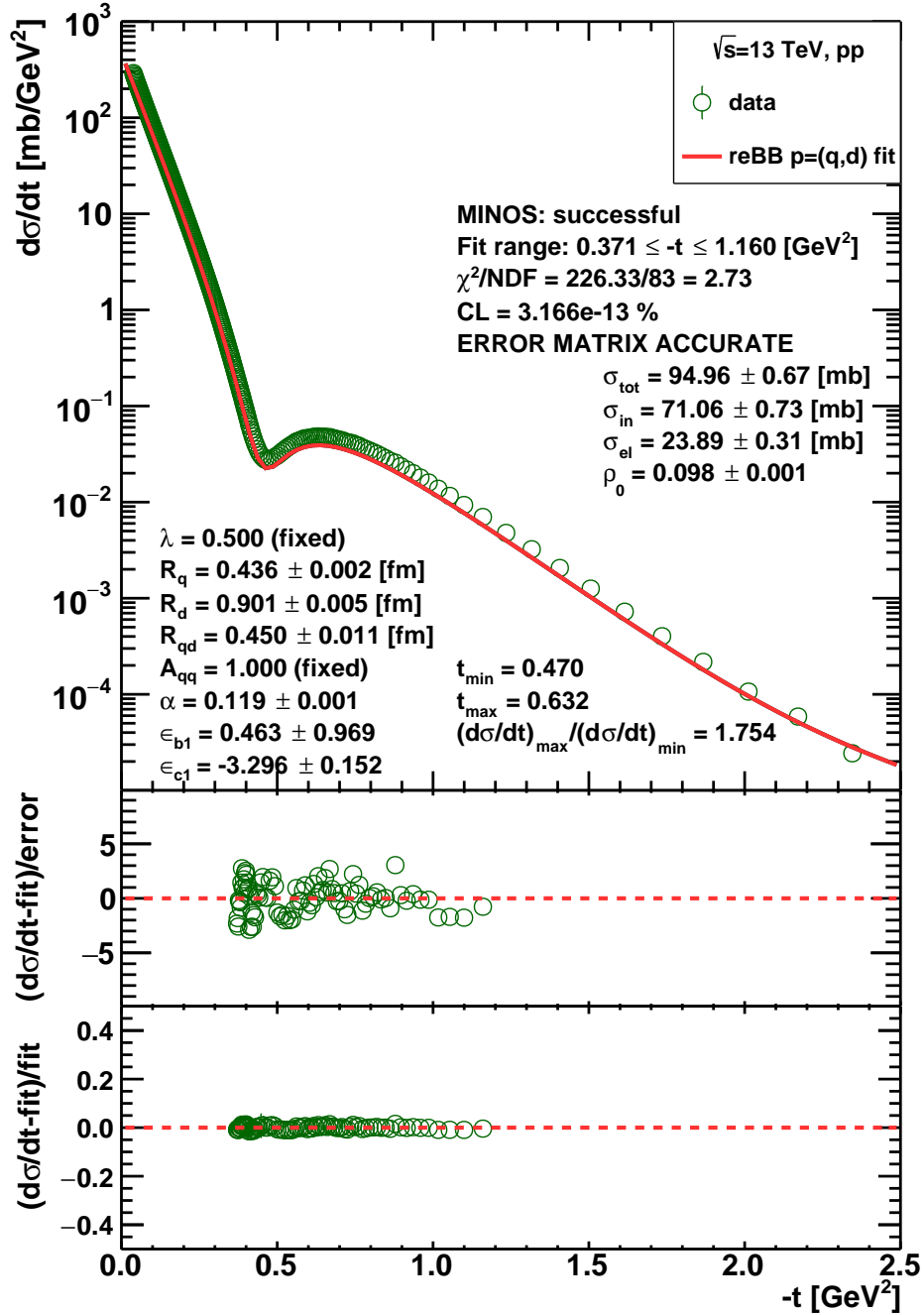


FIG. 5. The fit of the ReBB model to the pp TOTEM $\sqrt{s} = 13$ TeV data in the range of $0.37 \leq -t \leq 1.2$ GeV^2 [8]. The fit includes the t -dependent statistical (type A) and systematic (type B) uncertainties, the normalization (type C) uncertainty and the experimental values of the total cross section and parameter ρ with their full error according to Eq. (6). The fit parameters do not represent the data in a statistically acceptable manner, given that $\text{CL} \ll 0.1\%$. Otherwise, same as Fig. 1.

TABLE I. The values of the fitted ReBB model parameters to pp and $p\bar{p}$ data from SPS to LHC energies. The errors and the values are rounded up to three valuable decimal digits. For 7 TeV, the parameter error values shown in parenthesis do not include the contribution from the parameter correlations, i.e., are less than the MINOS errors.

\sqrt{s} [TeV]	0.546 ($p\bar{p}$)	1.960 ($p\bar{p}$)	2.760 (pp)	7.000 (pp)
$ t $ [GeV^2]	(0.375, 1.210)	(0.380, 1.200)	(0.372, 0.741)	(0.377, 1.205)
χ^2/NDF	44.49/33	8.22/9	17.32/16	80.29/52
CL [%]	8.74	51.12	36.52	0.713
R_q [fm]	0.349 ± 0.003	0.396 ± 0.006	0.419 ± 0.011	0.438 ± 0.005 (± 0.001)
R_d [fm]	0.825 ± 0.004	0.869 ± 0.012	0.877 ± 0.014	0.920 ± 0.009 (± 0.002)
R_{qd} [fm]	0.284 ± 0.010	0.294 ± 0.029	0.197 ± 0.084	0.333 ± 0.026 (± 0.002)
α	0.117 ± 0.002	0.163 ± 0.005	0.126 ± 0.006	0.122 ± 0.002 (± 0.001)
ϵ_{b1}	–	–	-0.094 ± 0.946	0.001 ± 0.003
ϵ_{c1}	-0.398 ± 0.911	-0.013 ± 0.834	0.059 ± 0.985	-0.091 ± 0.866
ϵ_{c2}	-0.090 ± 0.416	–	–	–

V. EXCITATION FUNCTIONS OF THE FIT PARAMETERS

In this section we determine the energy dependence of model parameters resulted from the above fits and summarized in Table I. The energy dependence of the scale parameters, R_q , R_d , and R_{qd} are shown in Figs. 6a-6c. These figures indicate that the energy dependence of the geometrical scale parameters, R_q , R_d and R_{qd} is consistent with the same evolution, namely the same linear rise in $\ln(s)$ for both pp and $p\bar{p}$ scattering: when we fitted these parameters together, with a linear logarithmic function, we have obtained a statistically acceptable fit in each of these three cases. This result extends and improves the earlier results published in ref. [36] for elastic pp scattering to the case of both pp and $p\bar{p}$ collisions in a natural manner.

Namely, we fit the s -dependence of the model parameters one by one, using the affine linear logarithmic function,

$$P(s) = p_0 + p_1 \cdot \ln(s/s_0), \quad P \in \{R_q, R_d, R_{qd}, \alpha\}, \quad (10)$$

where p_0 and p_1 are free parameters, s_0 is fixed to 1 GeV². We obtain good quality fits, with methods and results similar to that of ref. [36], with confidence levels $CL \gg 0.1\%$, as detailed in Table II.

We observe that in case of the geometrical scale parameters R_q , R_d and R_{qd} all the four data points (two pp and two $p\bar{p}$ points) follow within experimental errors approximately the same affine-linear function of $\ln(s)$ hence such a linear fit to four points is a non-trivial result, see panels (a)-(c) of Fig. 6. Actually the trends that are obtained are improving on similar earlier results that were obtained from ReBB model fits at the ISR energies of $\sqrt{s} = 23.5 - 62.5$ GeV and the elastic differential cross-section at $\sqrt{s} = 7$ TeV in ref. [36]. For a comparison, these earlier results are also shown with a dotted red line on the panles of Fig. 6, indicating the improved precision of the current analysis, due to more data points in the TeV energy range.

However, for the opacity parameter α we see on panel (d) of Fig. 6, that the pp and $p\bar{p}$ points are not on the same trend, because the α parameters that characterize the dip in the ReBB model, are obtained with great precision both in the pp and in the $p\bar{p}$ cases. The difference between the excitation functions of $\alpha^{pp}(s)$ and $\alpha^{p\bar{p}}(s)$ corresponds to the

qualitative difference between the differential cross-section of elastic pp and $p\bar{p}$ collisions in the few TeV energy range: the presence of a persistent dip and bump structure in the differential cross-section of elastic pp collisions, and the lack of a similar feature in elastic $p\bar{p}$ collisions. Here we have to consider, that there are only two, rather precisely determined data points for the value of the parameter α in both pp and $p\bar{p}$ collisions from the presented ReBB model studies so far. We can already conclude that they cannot be described by a single line as an affine linear fit with eq. (10) would fail, but without additional information, we cannot determine the trends and its uncertainties as two points can always be connected with a straight line, so an affine linear description of both the two pp and the two $p\bar{p}$ datapoints would have a vanishing χ^2 and an undeterminable confidence level. This problem is solved in A by adding new datapoints to the trends of $\alpha(s)$ both for the pp and for the $p\bar{p}$ cases, and the key point of the solution to this problem is summarized on Fig. 7, that shows that this fit parameter $\alpha(s)$ of the ReBB model is proportional to the real-to-imaginary ratio ρ and the constant of proportionality in the few TeV region is an almost energy independent constant value, $\rho/\alpha = 0.85 \pm 0.01$ is a constant, well within the errors of the $\rho \equiv \rho_0$ measurements, in agreement with a theoretically obtained function, showed with a red solid line on Fig. 7, that is derived in A. We found three additional published experimental data of ρ for $p\bar{p}$ collisions, $\rho = 0.135 \pm 0.015$ at $\sqrt{s} = 0.541$ by the UA4/2 Collaboration in ref. [62] and 1.8 TeV by the E-710 and the E811 collaborations in refs. [63, 64], respectively. At $\sqrt{s} = 1.8$ TeV, we have utilized the combined value of these E-710 and E811 measurements [64], corresponding to $\rho(p\bar{p}) = 0.135 \pm 0.044$. The constancy of these $\rho(s)$ values in the few TeV energy range, when converted with the help of Fig. 7 to the opacity parameter $\alpha(p\bar{p})$ of the Bialas-Bzdak model, leads to the lack of diffractive minima hence an Odderon signal in elastic $p\bar{p}$ collisions, leading to an $\alpha(p\bar{p}) \approx 0.16 \pm 0.06$ which is within its large errors the same as the $\alpha = 0.163 \pm 0.005$ value obtained from the ReBB model fit to D0 data at $\sqrt{s} = 1.96$ TeV, summarized on Fig. 2. Similarly the α parameter extracted from ρ at $\sqrt{s} = 0.541$ TeV is $\alpha \approx 0.16 \pm 0.02$ which is within twice the relatively large errors of the ρ analysis the same as the value of $\alpha(p\bar{p}) = 0.117 \pm 0.002$ obtained from the analysis of the differential cross-section, shown on Fig. 1. These indicate a slowly rising value for $\alpha(p\bar{p})$ or correspondingly, $\rho(p\bar{p})$ in the TeV energy. The final values of these datapoints together with the corresponding errors are connected with a long-dashed line in Panel (d) of Fig. 6. Table II indicates that for $\alpha(p\bar{p})$ the coefficient $p_1(p\bar{p}) = 0.018 \pm 0.002$ is a significantly positive number.

For the opacity coefficient in elastic pp collisions, $\alpha(pp)$ on the other hand an opposite effect is seen, when the ρ measurements at $\sqrt{s} = 7$ and 8 TeV are also taken into account, based on the data of the TOTEM Collaboration published in refs. [60, 65]. As by now it is very well known, these values indicate a nearly constant, actually decreasing trend, and based on the fits of the extracted four data points of $\alpha(pp)$ we find that in the few TeV energy range, this trend is nearly constant, indicated by the solid red line of Panel (d) of Fig. 6. Table II indicates that for $\alpha(pp)$ the coefficient of increase with $\ln(s)$ is consistent with zero in this energy range, $p_1(pp) = -0.003 \pm 0.003$, which is significantly less from the above quoted positive number for $p_1(p\bar{p}) = 0.018 \pm 0.002$. Based on their difference, we see that the Odderon signal in this analysis can be estimated to be an at least $6 - 7\sigma$ effect, based alone on the difference of the slope of the opacity or dip parameter, and the inequality $p_1(pp) \neq p_1(p\bar{p})$.

In what follows, we proceed carefully to determine the significance of this model dependent Odderon signal.

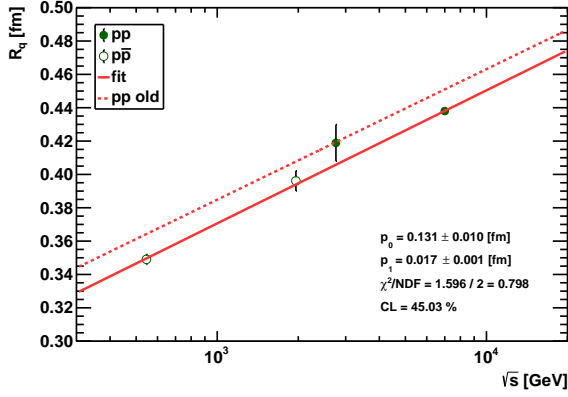
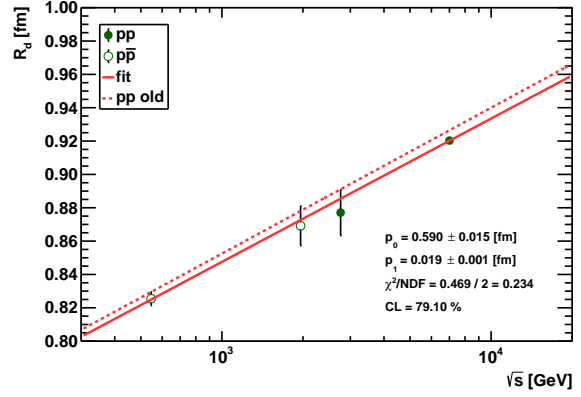
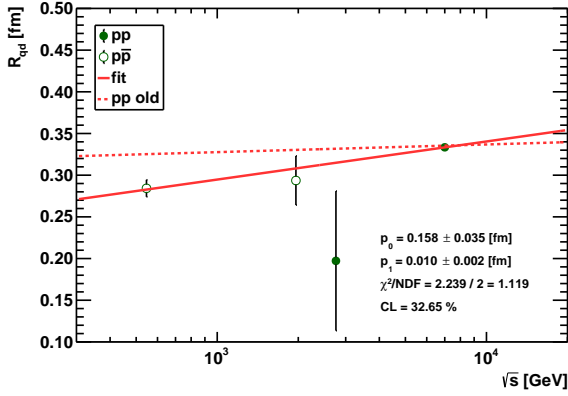
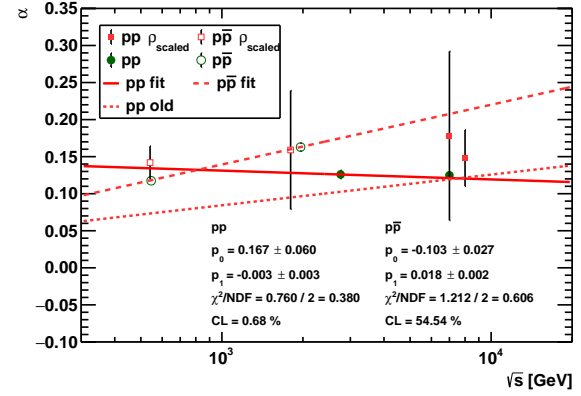
(a) Parameter R_q (b) Parameter R_d (c) Parameter R_{qd} (d) Parameter α

FIG. 6. The energy dependence of the parameters of the ReBB model, R_q , R_d , R_{qd} and α , collected in Table I and determined by fitting a linear logarithmic model, Eq. (10), to each of them one by one.

TABLE II. Summary of the parameter values which determine the energy dependence according to Eq. (10). The values of the parameters are rounded up to three valuable decimal digits.

Parameter	R_q [fm]	R_d [fm]	R_{qd} [fm]	α (pp)	α (p-pbar)
χ^2/NDF	1.596/2	0.469/2	2.239/2	0.760/2	1.212/2
CL [%]	45.03	79.10	32.65	0.68	54.54
p_0	0.131 ± 0.010	0.590 ± 0.015	0.158 ± 0.035	0.167 ± 0.060	-0.103 ± 0.027
p_1	0.017 ± 0.001	0.019 ± 0.001	0.010 ± 0.002	-0.003 ± 0.003	0.018 ± 0.002

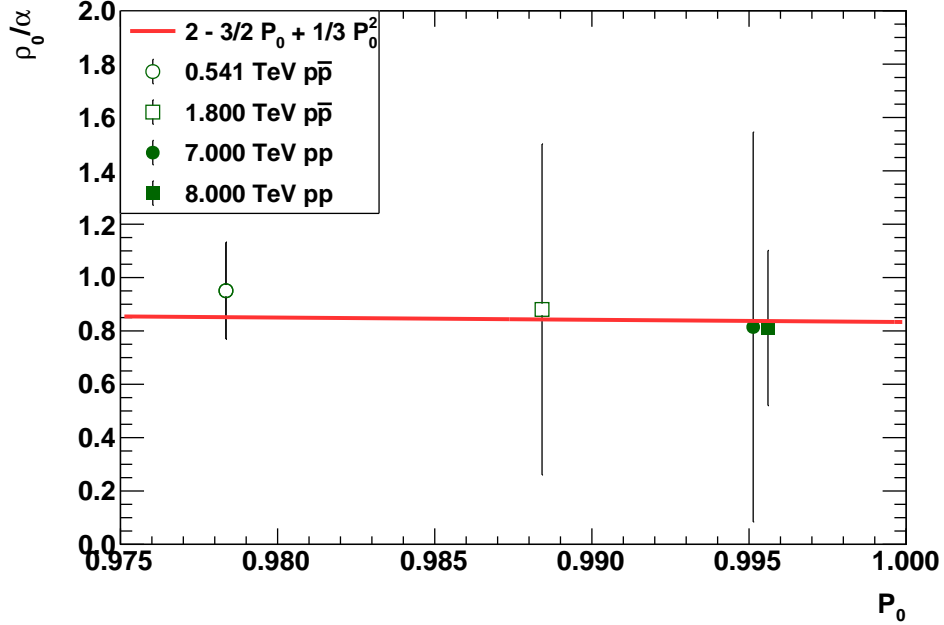


FIG. 7. The dependence of ρ_0/α on P_0 in the TeV energy range. The data points are generated numerically by using the trends of the ReBB model parameters, R_q , R_d , R_{qd} , shown in Figs. 6a-6c and the experimentally measured ρ -parameter values. The red curve represents the result of the analytical calculation showing a good agreement with the numerical calculations.

In the subsequent sections, we first perform cross-checks called sanity tests: we test if the excitation functions, determined with the help of the p_0 and p_1 parameters of Table II indeed reproduce the data at various measured energies. We perform these cross-checks against all kind of available data, including those data that were not utilized in the determination of the trends for example because their acceptance was too limited to determine all the fit parameters of the ReBB model. Of course we also cross-check in this sanity test section of VI, if the trends obtained and summarized in Table II reproduce, with a statistically acceptable $CL \geq 0.1\%$, also those datasets that were utilized to establish the trends. After the successful sanity tests, we are ready to extrapolate pp data from the LHC energies of $\sqrt{s} = 2.76$ and 7.0 TeV to the top Tevatron energy of 1.96 TeV, and vice versa. These extrapolations are our main results and they are presented in Section VII. Additionally we discuss possible non-linearities and their effects on the Odderon signal in Section VIII.

The fits to the excitation function of the ReBB model parameters are shown in panels (a)-(c) of Fig. 6 and a similar fit to the excitation functions of the ReBB model parameter

α , together with α values obtained from other ρ measurements with the method A are presented in panel (d) of the same figure. The fit parameters of these excitation functions are collected and summarized in Table II.

VI. SANITY TESTS

In this section we show that the determined energy dependence trends are reliable. For this purpose we performed the so-called sanity tests: we have cross-checked that the trends summarized in Table II indeed represent the differential cross-sections of both pp and $p\bar{p}$ elastic scattering in the few TeV energy range, where such data are available?

Thus in this section, the differential cross sections are fitted with all the four physical parameters the ReBB model: $\alpha(s)$, $R_q(s)$, $R_d(s)$ and $R_{qd}(s)$ are fixed to their extrapolated value obtained with the help of the results summarized in Table II, while the correlation coefficients of the type B and C errors, or the ϵ parameters in the χ^2 definition of eq. (6) are fitted to the data as free parameters.

The results for the data at $\sqrt{s} = 0.546, 0.63, 1.8, 1.96, 2.76$ and 7 TeV are shown in Figs. 8-13. All of these sanity tests resulted in the description of these data with a statistically acceptable confidence level of CL ≥ 0.1 %.

As an additional sanity test, we have also cross-checked if this ReBB model describes the pp and $p\bar{p}$ total cross section $\sigma_{\text{tot}}(s)$ and real to imaginary ratio $\rho(s)$ data in a statistically acceptable manner, or not. These results are presented on Figs. 14 and Fig. 15, respectively. As the calculated confidence levels are higher than 0.1 % in all of these cases, we can happily conclude that the energy dependent trends of the ReBB model are really reasonable and reliable in the investigated $0.541 \leq \sqrt{s} \leq 8$ TeV energy and in the $0.377 \leq -t \leq 1.2$ GeV² four-momentum transfer range. Thus this model can be used reliably to extrapolate both the pp and the $p\bar{p}$ differential cross-sections in this limited kinematic range.

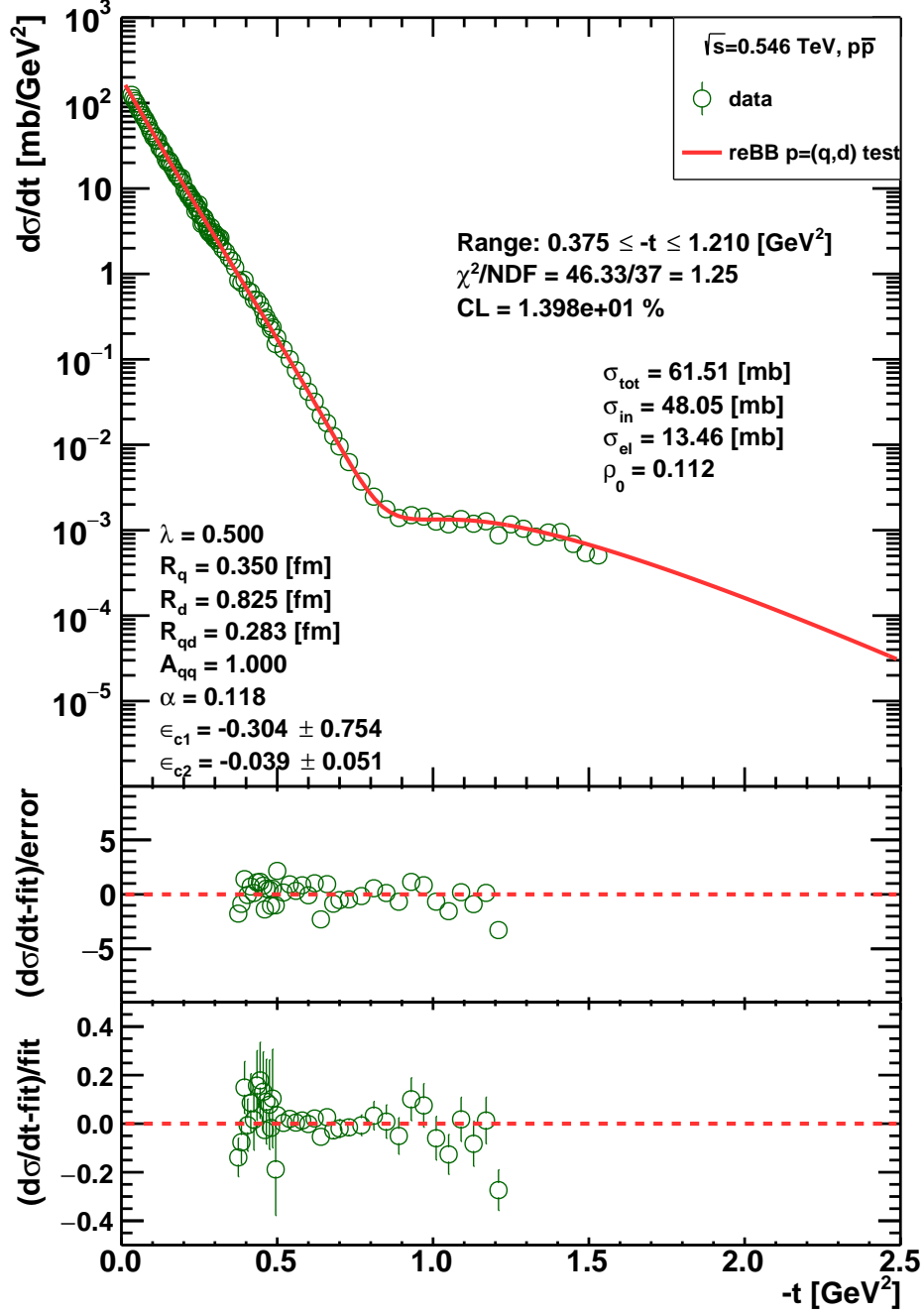


FIG. 8. Result of the sanity test for the 0.546 TeV $p\bar{p}$ elastic differential cross section data [51, 52] in the range of $0.37 \leq -t \leq 1.2$ GeV². This sanity test was performed as a fit during which the model parameters R_q , R_d , R_{qd} and α were fixed to their s -dependent value based on Table II, while correlation coefficients ϵ -s in the χ^2 definition, Eq. (6), were fitted as free parameters. The parameter values are rounded up to three valuable decimal digits.

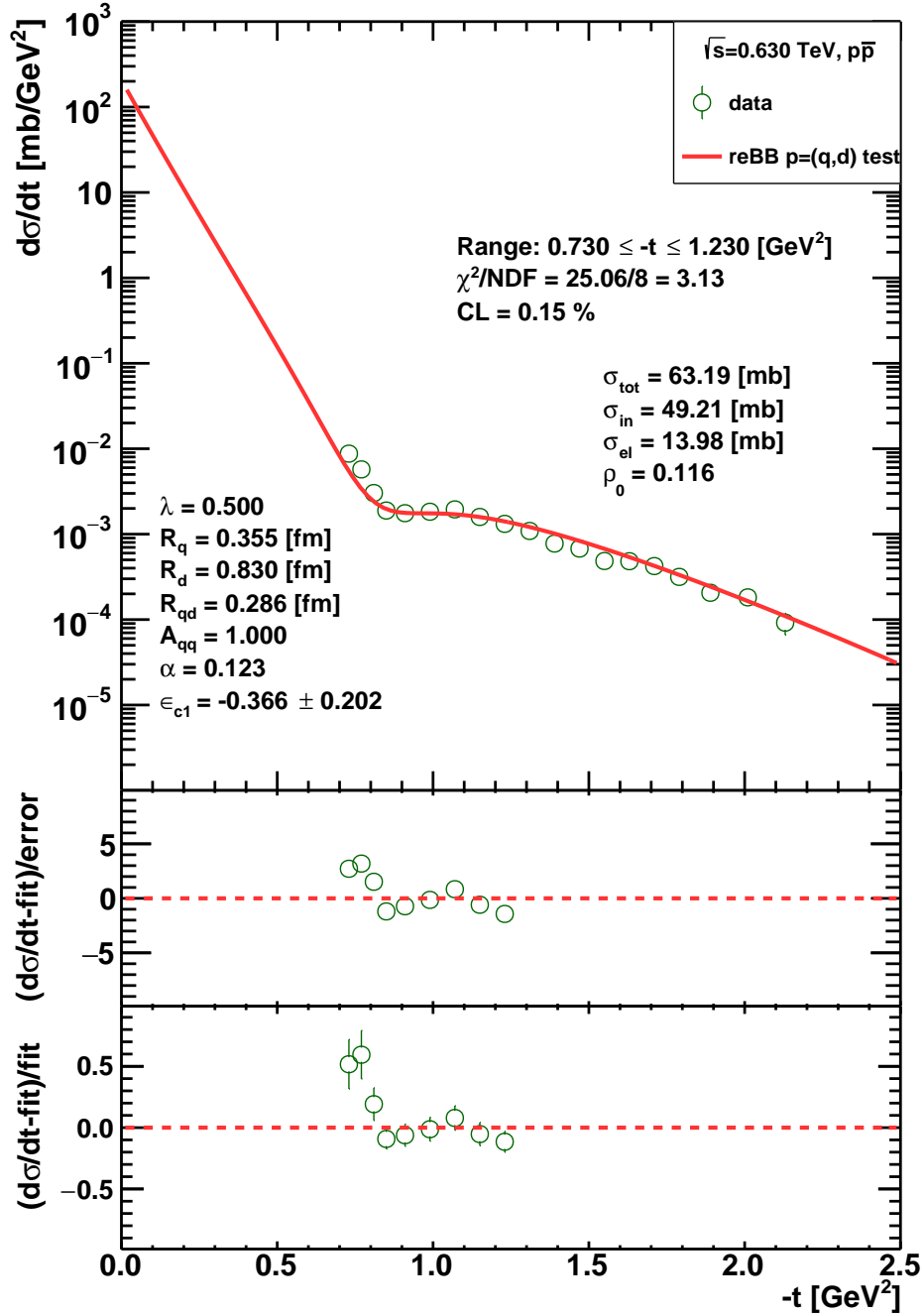


FIG. 9. Result of a sanity test, similar to Fig. 8, but for the $\sqrt{s} = 0.63 \text{ TeV}$ $p\bar{p}$ elastic differential cross section data of ref. [66], fitted in the range $0.7 \leq -t \leq 1.2 \text{ GeV}^2$.

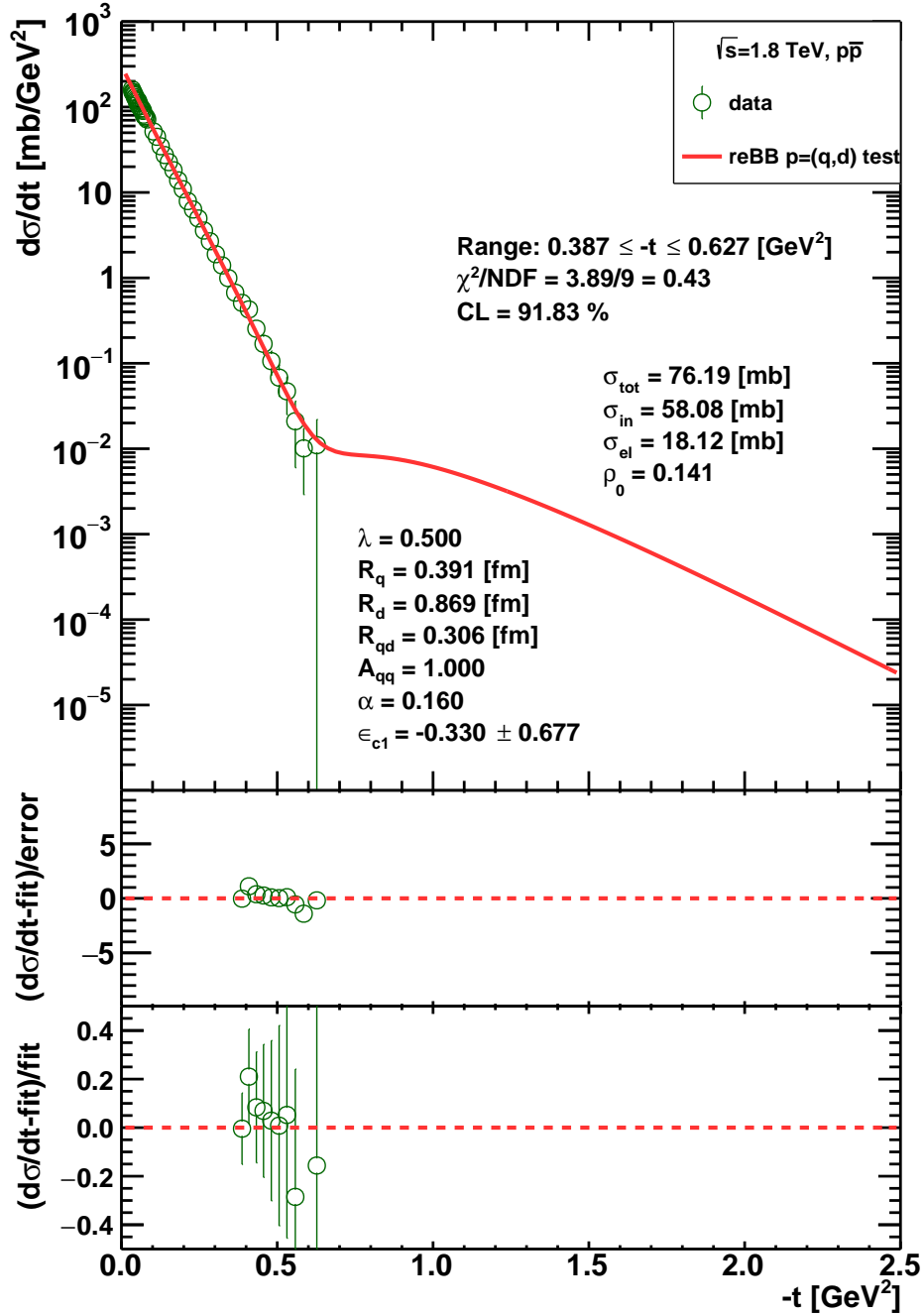


FIG. 10. Result of a sanity test, same as Fig. 8, but for the 1.8 TeV $p\bar{p}$ elastic differential cross section data [67] in the range of $0.37 \leq -t \leq 0.6 \text{ GeV}^2$.

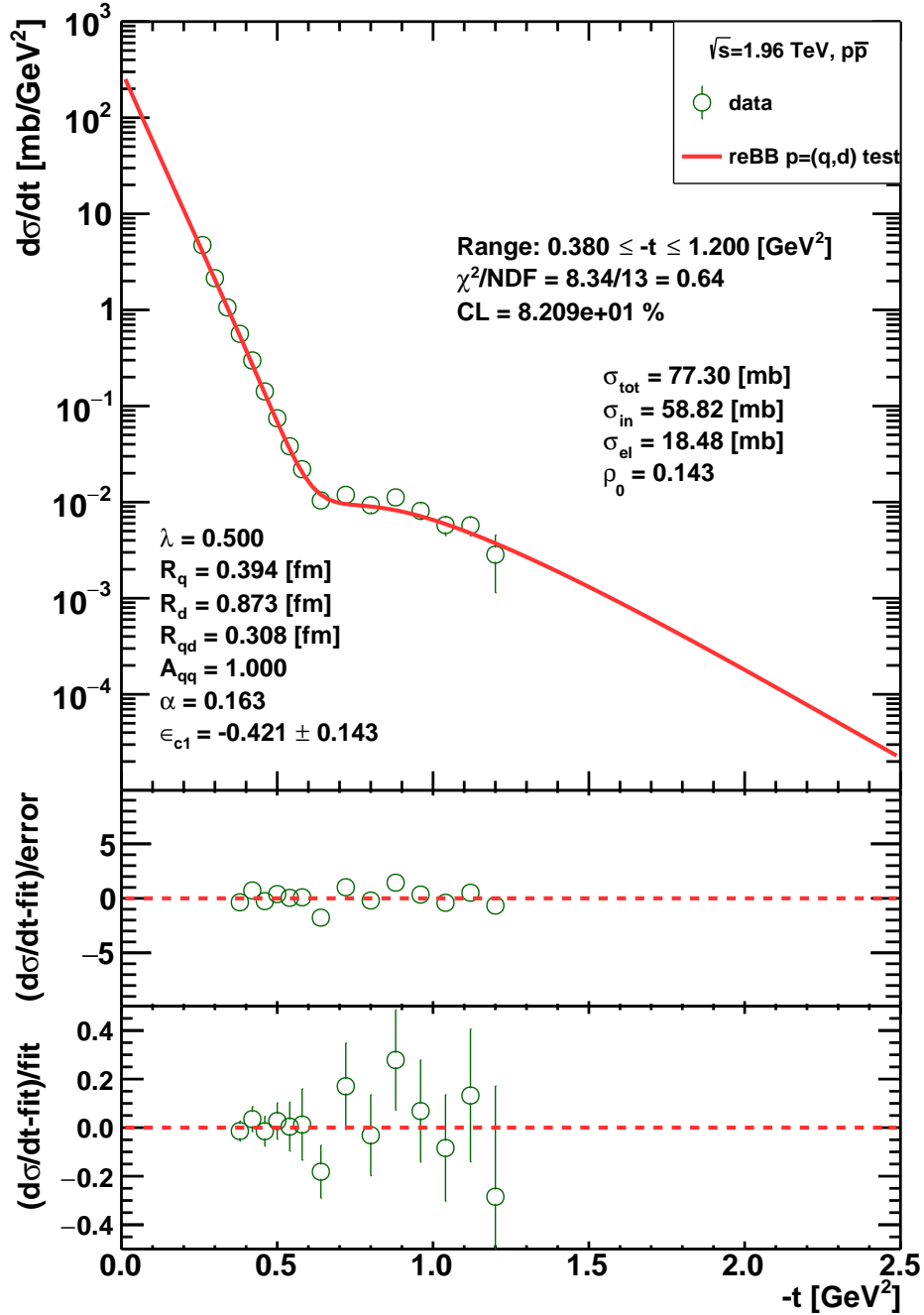


FIG. 11. Result of a sanity test, same as Fig. 8, but for the $\sqrt{s} = 1.96 \text{ TeV}$ $p\bar{p}$ elastic differential cross section data [53] in the range of $0.37 \leq -t \leq 1.2 \text{ GeV}^2$.

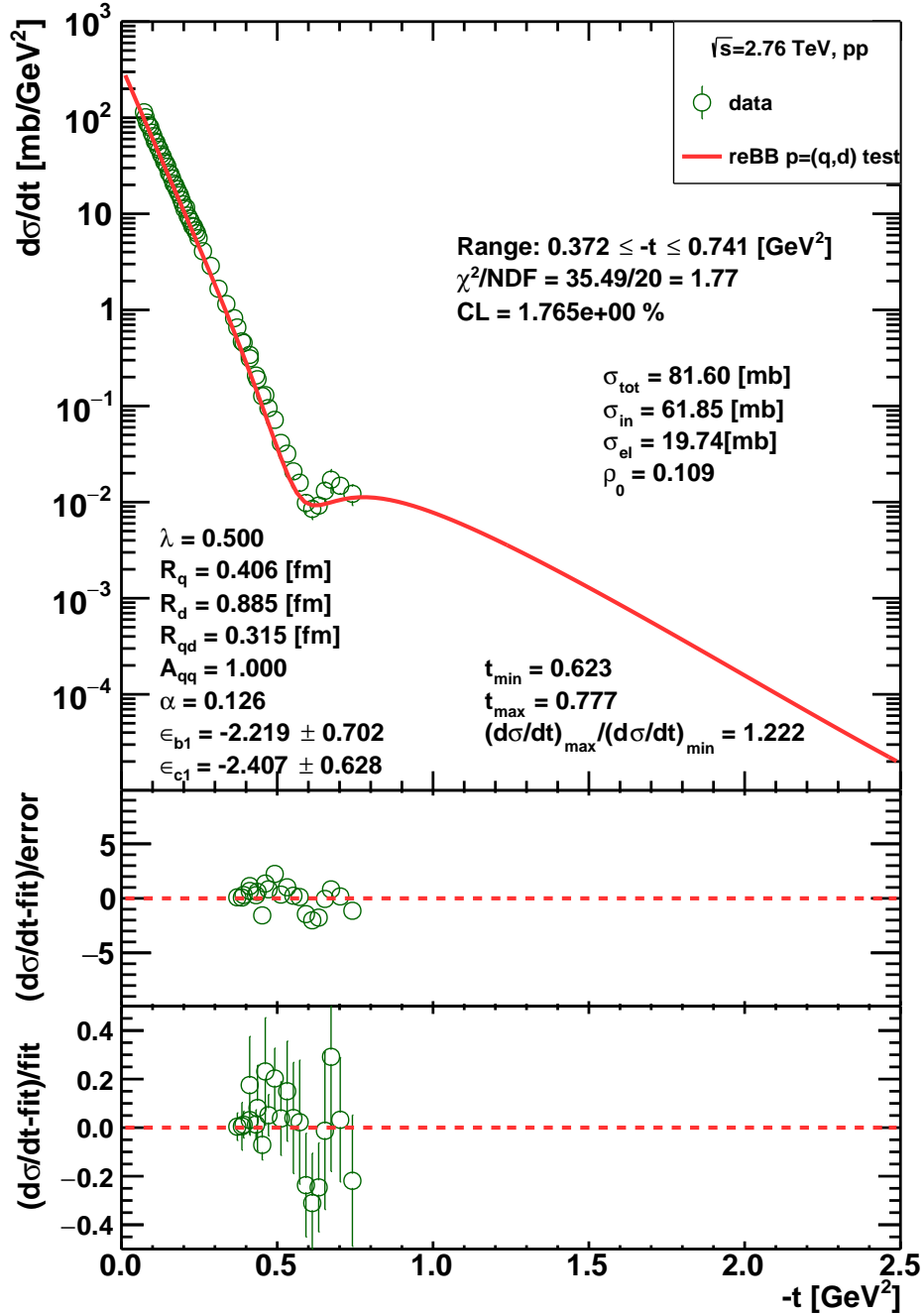


FIG. 12. Result of a sanity test, same as Fig. 8, but for the $\sqrt{s} = 2.76$ TeV pp elastic differential cross section data [9] in the range of $0.37 \leq -t \leq 0.7$ GeV².

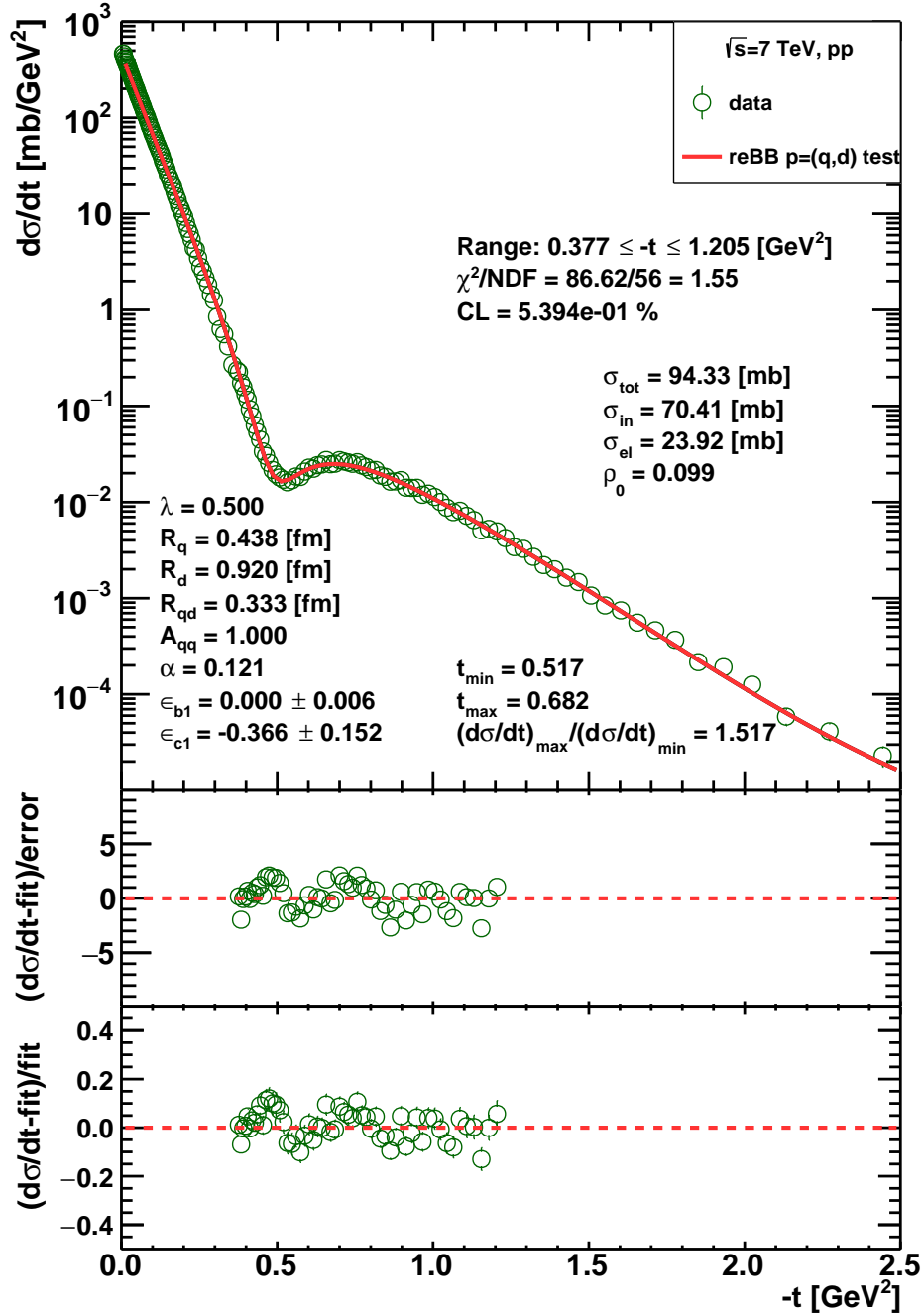


FIG. 13. Result of a sanity test, same as Fig. 8, but for the pp elastic differential cross section data at $\sqrt{s} = 7$ TeV from ref. [50], in the fitted range of $0.37 \leq -t \leq 1.2\text{GeV}^2$.

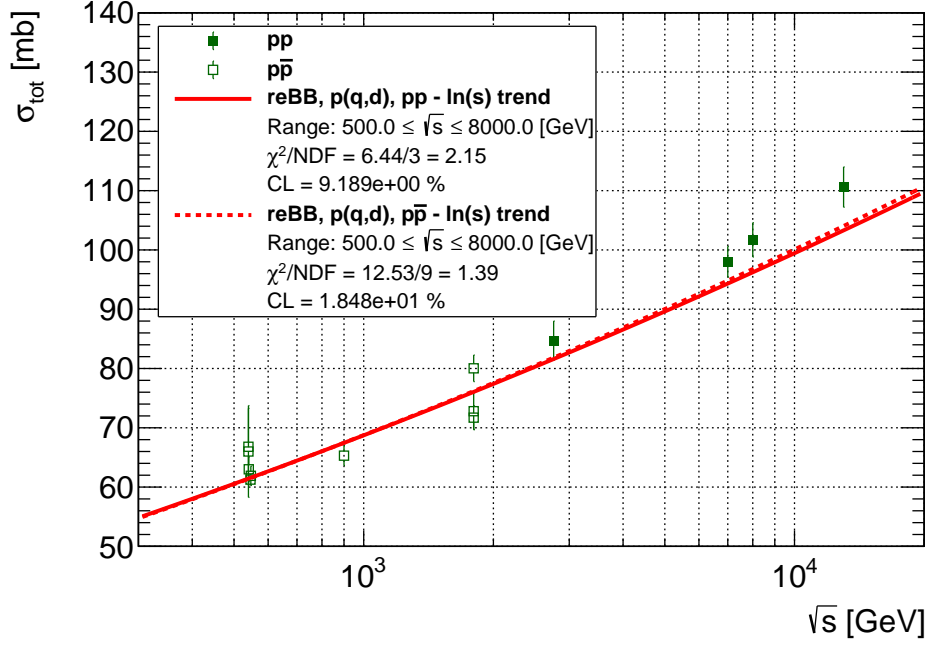


FIG. 14. Result of the sanity test for pp [6, 65, 68] and $p\bar{p}$ [54] total cross section data. It was calculated from the model when the values of the parameters R_q , R_d , R_{qd} and α were taken from the trends, corresponding to panels (a)-(d) of Fig.6.

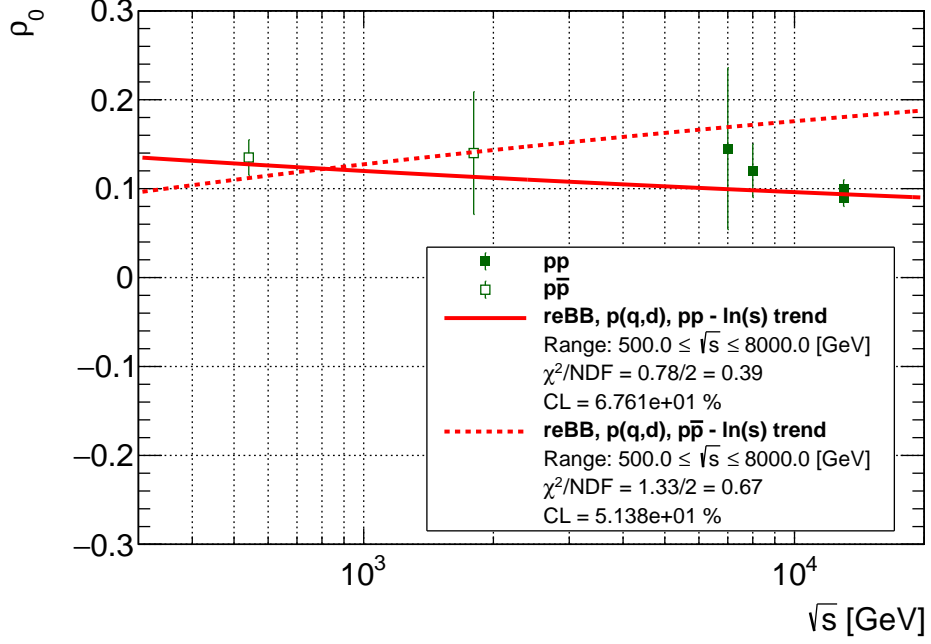


FIG. 15. Sanity test result for pp [7, 60, 65] and $p\bar{p}$ [54] parameter ρ data. It was calculated from the model when the values of the parameters R_q , R_d , R_{qd} and α were taken from the trends, corresponding to panels (a)-(d) of Fig.6. On this plot, a model dependent Odderon effect is clearly identified: it corresponds to the difference between the excitation functions of ρ for pp and for $p\bar{p}$ collisions. In particular, the trend of ρ for $p\bar{p}$ collisions deviates significantly from the data for pp collisions.

VII. EXTRAPOLATIONS

According to our findings in Section V the energy dependence of the scale parameters R_q , R_d and R_{qd} are identical for pp and $p\bar{p}$ scattering, only the energy dependence of the opacity parameter α differs. The statistically acceptable quality of the fits shown in Fig. 6 and the success of the sanity tests performed in the previous section allow for a reliable extrapolation of the differential cross-sections of elastic pp and $p\bar{p}$ collisions with the help of the ReBB model [36], limited to the investigated $0.541 \leq \sqrt{s} \leq 8$ TeV center of mass energy and in the $0.377 \leq -t \leq 1.2$ GeV² four-momentum transfer range.

In this section, we present the results of such pp extrapolations to energies where measured $p\bar{p}$ data exist and the other way round, $p\bar{p}$ extrapolations to energies where measured pp data exist. During these extrapolations, the values of the scale parameters R_q , R_d and R_{qd} and that of the opacity parameter α are fixed to their values on their corresponding trends, summarized on Fig. 6d and in Table II. These extrapolations were performed as fits, where the model parameters R_q , R_d , R_{qd} and α were fixed while the correlation coefficients, the ϵ parameters in the χ^2 definition, Eq. (6) were optimized. In this procedure, the two last two terms in Eq. (6), i.e., the total cross section and ρ -parameter term, were not included. This way we handled the type B and type C errors of the published pp differential cross-section to match these data as much as possible to the differential cross-section of elastic $p\bar{p}$ collisions within the allowed systematic errors as much as possible, and vice versa.

Three of such extrapolations were performed: pp extrapolation to $\sqrt{s} = 1.96$ TeV, to compare it to the 1.96 TeV D0 $p\bar{p}$ $d\sigma/dt$ data, and $p\bar{p}$ extrapolations to $\sqrt{s} = 2.76$ and 7 TeV, to compare them to the $d\sigma/dt$ pp data measured by TOTEM at these energies. The error band around these extrapolations is also evaluated, based on the envelope of one standard deviation errors of the p_0 and p_1 parameters of the four physical model parameters $R_q(s)$, $R_d(s)$, $R_{qd}(s)$ and $\alpha(s)$.

The results are shown in Fig. 16, Fig. 17 and Fig. 18. While at $\sqrt{s} = 1.96$ TeV no significant difference is observed between the extrapolated pp and measured $p\bar{p}$ differential cross sections, at $\sqrt{s} = 2.76$ and 7 TeV, remarkable and statistically significant differences can be observed.

On these Figures, even an untrained eye can see, that the dip is filled in case of elastic $p\bar{p}$ scattering, while it is not filled in elastic pp scattering. Thus we confirm the prediction of

ref. [48], that predicted, based on a three-gluon exchange picture that dominates at larger values of $-t$, that the dip will be filled in high energy $p\bar{p}$ elastic collisions.

In this work, the differences between elastic pp and $p\bar{p}$ collisions are quantified by the confidence levels obtained from the comparison of these extrapolated to the measured data: at 2.76 TeV, the hypothesis that these extrapolations agree with the data is characterized by a $CL = 1.092 \times 10^{-10}$ %, while at 7 TeV, $CL = 0$ %. Theoretically the observed difference can be attributed only to the effect of a C-odd exchange, as detailed recently in refs. [30–32]. At the TeV energy scale, the secondary Reggeon exchanges are generally known to be negligible, an effect that has been also specifically cross-checked and confirmed recently in ref. [69]. Thus in the few TeV energy range of the LHC, the only source of a difference between the differential cross-sections of elastic pp and $p\bar{p}$ collisions can be a t -channel Odderon exchange. In the modern language of QCD, Odderon exchange corresponds to the exchange of a C-odd colorless bound states consisting of odd number of gluons [2, 48, 70].

Thus the CL, calculated for the 2.76 TeV $p\bar{p}$ extrapolation, corresponds to an Odderon observation with a probability of $P = 1 - CL = 1 - 1.092 \times 10^{-12}$. This corresponds to a 7.1 σ model dependent significance for the observation of a t channel Odderon exchange, and the existence of the colorless bound states containing odd number of gluons. This significance is even larger when the extrapolated $p\bar{p}$ differential cross-sections are compared to TOTEM elastic pp data measured at $\sqrt{s} = 7$ TeV, where the probability of Odderon observation becomes practically unity.

Let us note that we have also been recently involved in a truly model-independent search for Odderon effects in the comparison of the scaling properties of the differential cross-sections of elastic pp and $p\bar{p}$ collisions in a similar s but in the complete available t range. As compared to the model-dependent studies summarized in this manuscript, the advantage of the model-independent scaling studies of refs. [30–32] is that they scale out all the effects from the differences between pp and $p\bar{p}$ elastic collisions due to possible differences in their $\sigma_{\text{tot}}(s)$, $\sigma_{\text{el}}(s)$, $B(s)$ and $\rho(s)$ functions. As part of the Odderon signal in the ReBB model is apparently in the difference between the $\rho(s)$ excitation functions for pp and $p\bar{p}$ collisions, the significance of the Odderon signal is reduced in this model independent analysis. When considering the interpolations as theoretical curves, the significance is reduced to a 6.55 σ effect [30], but when considering that the interpolations between experimental data have also horizontal and vertical, type A and type B errors, the significance of the Odderon signal

is further reduced to a 6.26σ effect [31, 32]. Thus we conclude that the Odderon is now discovered, both in a model dependent and in a model-independent manner, with a statistical significance that is well above the 5σ discovery limit of high energy particle physics.

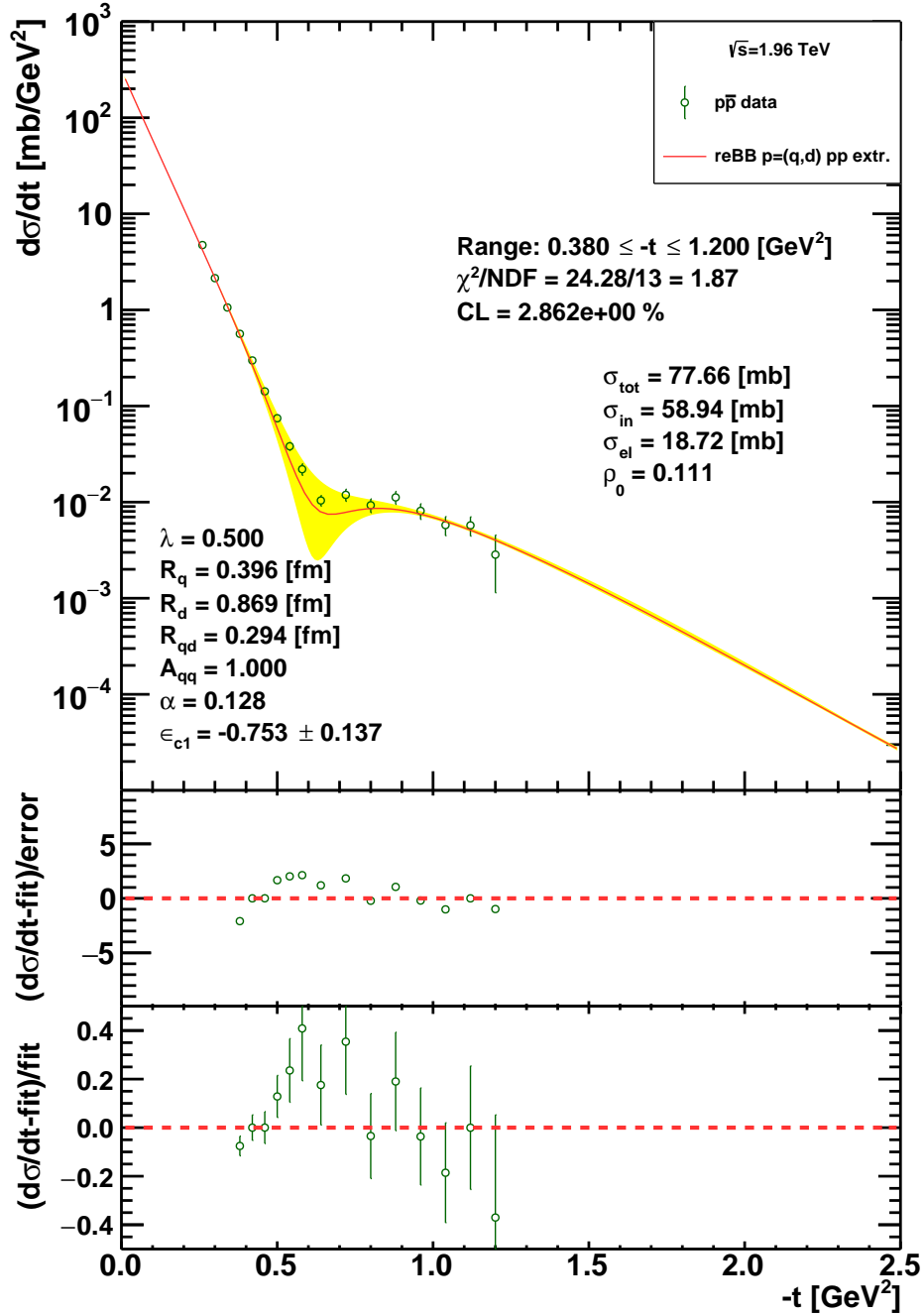


FIG. 16. The ReBB model extrapolation for the pp $d\sigma/dt$ at $\sqrt{s} = 1.96$ TeV compared to the $p\bar{p}$ D0 $d\sigma/dt$ data[53] measured the same energy. The yellow band is the uncertainty of the extrapolation. The calculated CL value between the extrapolated model and the measured data does not indicate a significant difference between the pp and $p\bar{p}$ differential cross sections.

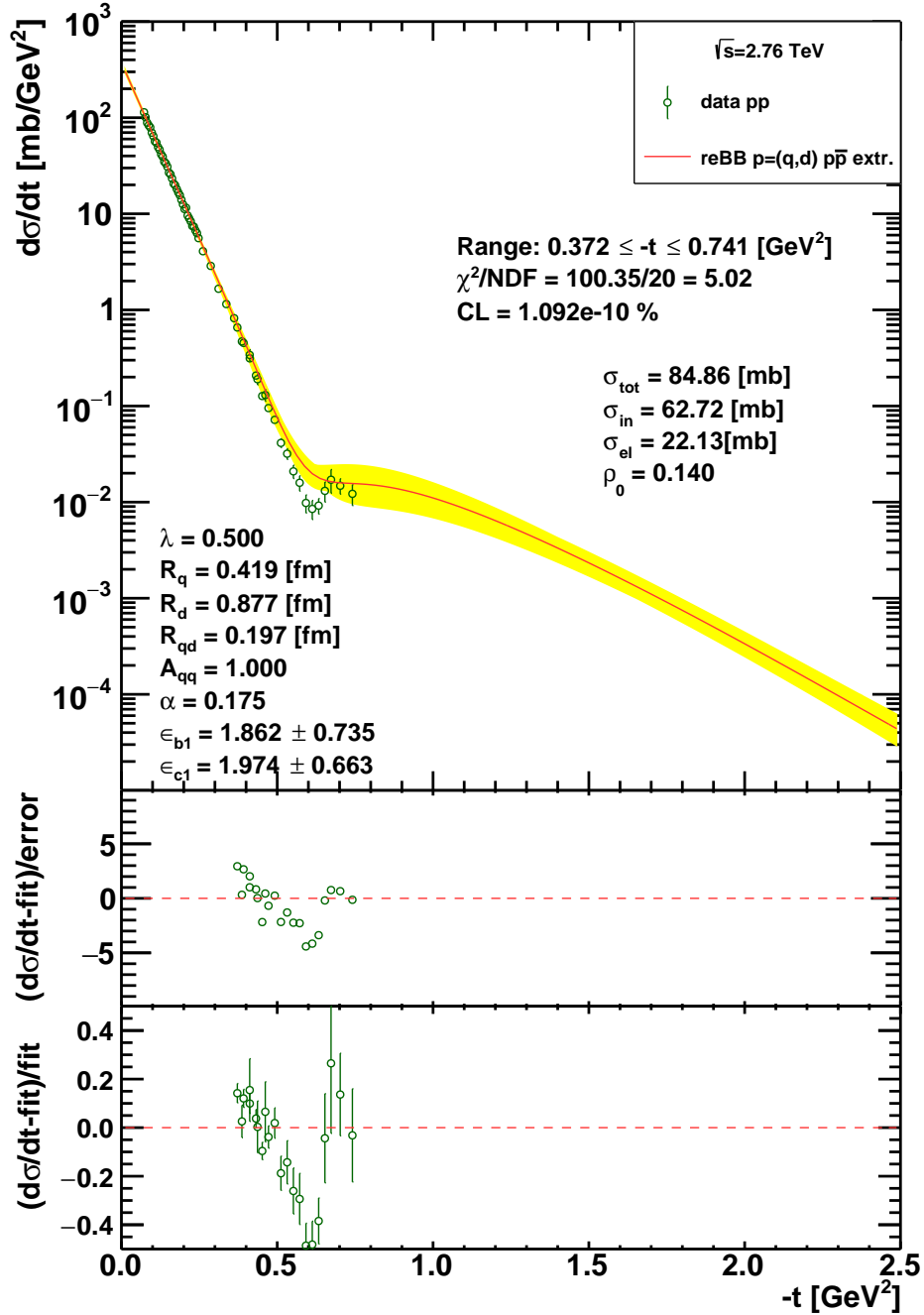


FIG. 17. The ReBB model extrapolation for the $p\bar{p}$ $d\sigma/dt$ at $\sqrt{s} = 2.76$ TeV compared to the pp TOTEM $d\sigma/dt$ data[9] measured at the same energy. The yellow band is the uncertainty of the extrapolation. The calculated CL value between the extrapolated model and the measured data indicates a significant difference between the pp and $p\bar{p}$ differential cross sections, corresponding to a 7.1σ significance for the t -channel Odderon exchange.

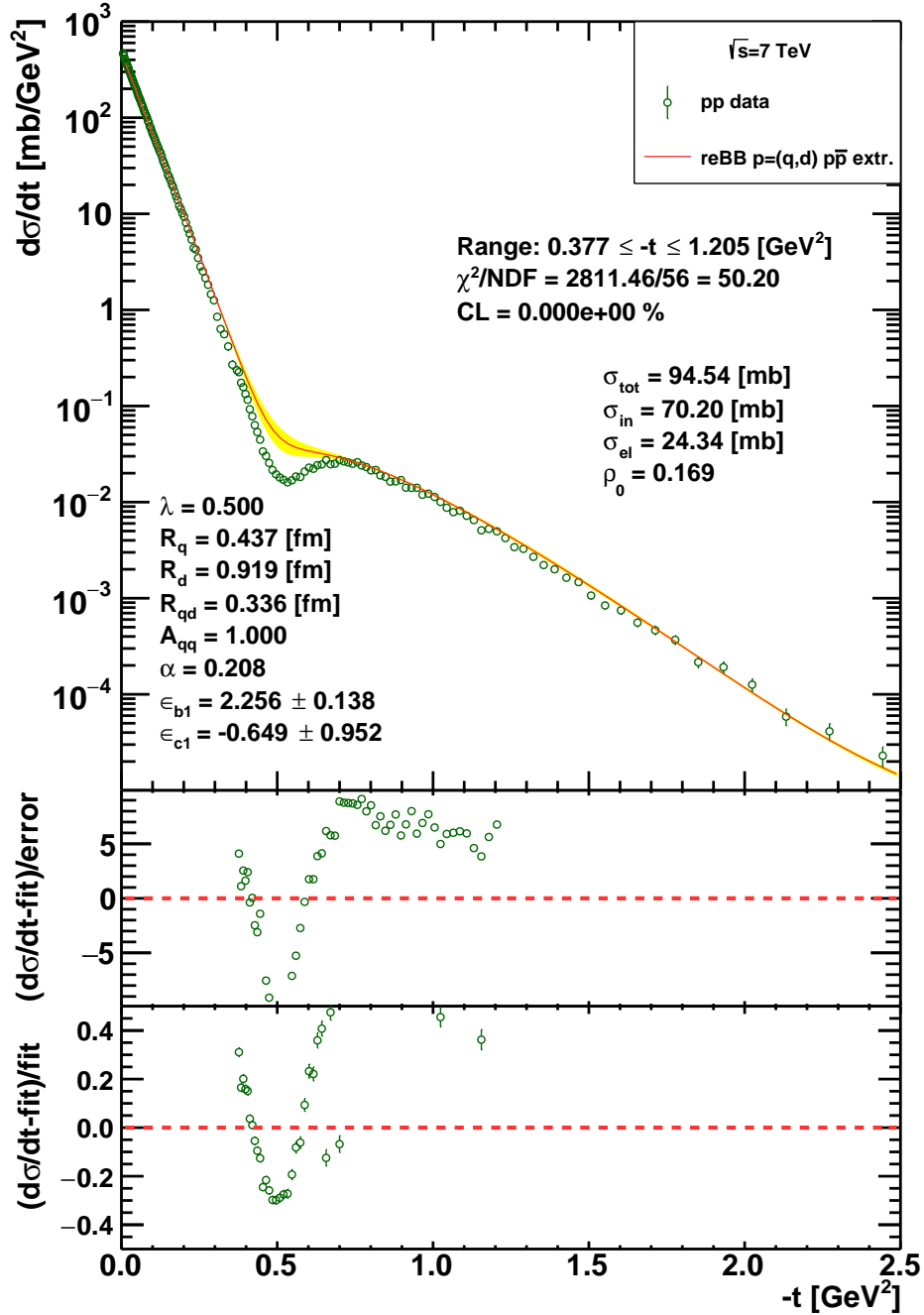


FIG. 18. The ReBB model extrapolation for the $p\bar{p}$ $d\sigma/dt$ at $\sqrt{s} = 7 \text{ TeV}$ compared to the pp TOTEM $d\sigma/dt$ data[50] measured at the same energy. The yellow band is the uncertainty of the extrapolation. The calculated CL value between the extrapolated model and the measured data indicates a significant difference between the pp and $p\bar{p}$ differential cross sections, hence a significant Odderon effect, that is dominant around the dip region.

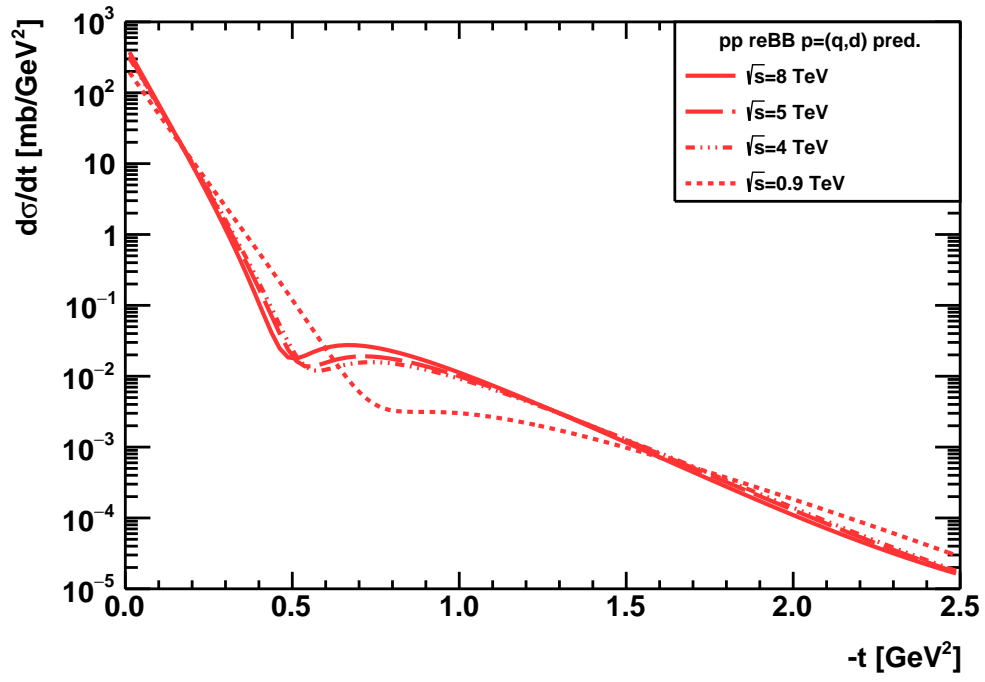


FIG. 19. Predictions from the ReBB model, for the $d\sigma/dt$ of elastic pp collisions at $\sqrt{s} = 8, 5, 4,$ and 0.9 TeV.

VIII. DISCUSSION

In the previous sections, we have investigated what happens if we interpret the data in terms of a particular model, the Real Extended Bialas-Bzdak Model. This allows also to consider Odderon signal in the excitation function of the model parameter α . We have shown in Appendix A that this model parameter is proportional to the experimentally measured parameter ρ , the ratio of the real to the imaginary part of the scattering amplitude at the optical point, and related the coefficient of proportionality to the value of the shadow profile function at vanishing impact parameter for the $\sqrt{s} \leq 8$ TeV elastic proton-proton collisions, and we have shown that within the framework of this ReBB model, the very different trend of $\rho(s)$ in proton-proton and in proton-antiproton collisions enhances the model-independent Odderon signal, from a 6.26 σ and 6.55 σ effect to a 7.1 σ effect.

Recently, the TOTEM Collaboration concluded, that only one condition is yet to be satisfied to see a statistically significant Odderon signal: namely, the logarithmically small energy gap between the lowest TOTEM energy of $\sqrt{s} = 2.76$ TeV at LHC and the highest D0 energy of 1.96 TeV at Tevatron needs to be closed. This energy gap has been closed in a model-independent way in refs. [30–32], using the scaling properties of elastic scattering, and by comparing the $H(x) = \frac{1}{B\sigma_{el}} \frac{d\sigma}{dt}$ scaling functions of elastic proton-proton and proton-antiproton collisions, as a function of $x = -tB$ at $\sqrt{s} = 1.96, 2.76$ and 7.0 TeV. The advantages of that method, with respect to comparing the cross sections directly include the scaling out of the s -dependencies of $\sigma_{tot}(s)$, $\sigma_{el}(s)$, $B(s)$ and $\rho(s)$, as well as the normalization of the $H(x)$ scaling function that cancels the point-to-point correlated and t -independent normalization errors. The validity of the $H(x)$ scaling for pp collisions and its violation in $p\bar{p}$ collisions in the few TeV energy range resulted in a discovery level statistical significance of an Odderon signal, characterized in refs. [30–32] to be at least 6.26 σ , model independently, based on a careful interpolation of the experimental data-points, their point-to-point fluctuating, point-to-point correlated and data point dependent as well as point-to-point correlated and data point independent errors. If these errors are considered as errors on a theory curve, then the significance goes up to at least 6.55 σ [30].

In high energy particle physics, the standard accepted discovery threshold corresponds to a 5 σ effect. In the previous section, we have shown, that the statistical significance of an Odderon observation in the limited $0.541 \leq \sqrt{s} \leq 8$ TeV center of mass energy and in the

$0.377 \leq -t \leq 1.2 \text{ GeV}^2$ four-momentum transfer range is at least 7.1σ , corresponding to a statistically significant and model dependent Odderon observation.

Detailing these results, in this section we investigate the stability of our result for the case, when the energy range is extended towards lower values of \sqrt{s} . In order to do this, we refitted the ISR data[71] at all the five available collision energy ($\sqrt{s} = 23.5, 30.7, 44.7, 52.8$ and 62.5 GeV) in the squared momentum transfer range $0.8 \leq -t \leq 2.5 \text{ GeV}^2$ by using the χ^2 definition determined by Eq. 6. The fits included the t -dependent (both vertical and horizontal) statistical (type A) and systematic (type B) errors, the normalization (type C) error and the experimental values of the total cross section and the parameter ρ with their total uncertainties [72]. We have also tested the stability of the fit results for small variations of the fit range or the fitting method. The only data set, where our results remained stable for the variation of the fit range around the selected range and for small variations of the fitting procedure, and where the obtained results were both statistically and physically acceptable fit results describing not only the differential cross-section but the measured value of the total cross-section σ_{tot} and the value of the real to imaginary ratio ρ was the ISR dataset, measured at $\sqrt{s} = 23.5 \text{ GeV}$. The result of this satisfactory fit is shown in Fig. 20. Our other results were similar to the results presented in ref. [36] and particularly resulted in a rather fluctuating description of the excitation function of the $\rho(s)$ at those ISR energies. In the present study we do utilize the experimental information on $\rho(s)$ so such fluctuating fits could not be used to establish the trends and the excitation functions. However, we cross-checked that the established trends do describe very well the excitation functions of $\rho(s)$, both in the ISR energy range, and in the LHC energy range, as indicated on Figs. 21, 22 and 7, respectively.

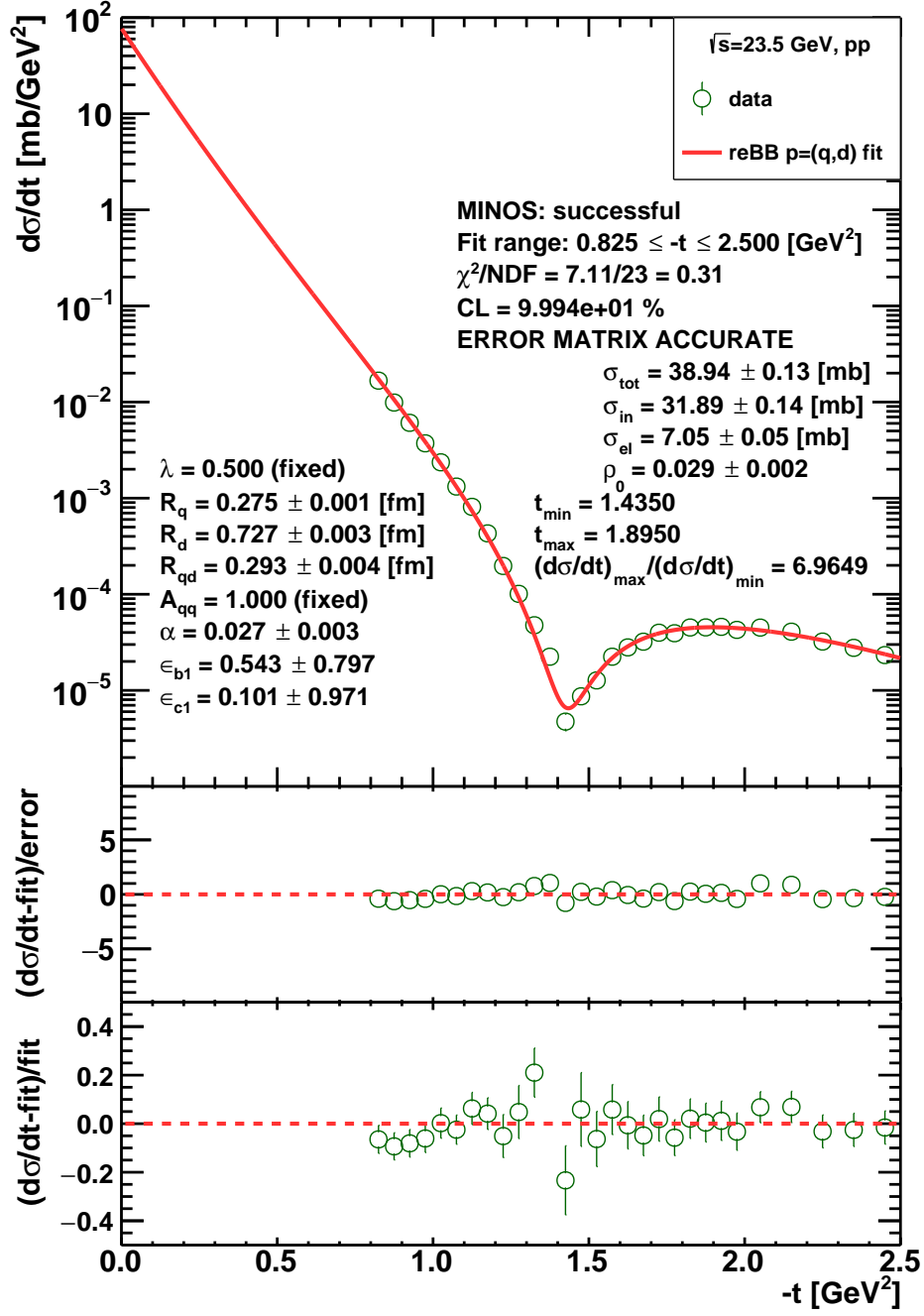


FIG. 20. The fit of the ReBB model to the pp ISR $\sqrt{s} = 23.5$ GeV data in the range of $0.8 \leq -t \leq 2.5$ GeV² [72]. The fit includes the t -dependent statistical (type A) and systematic (type B) uncertainties, the normalization (type C) uncertainty and the experimental values of the total cross section and parameter ρ with their full error according to Eq. (6). The fitted parameters are shown in the left bottom corner and their values are rounded up to three decimal digits.

We noticed that, when the $\sqrt{s} = 23.5$ GeV energy data are included to those summarized in Table I, the energy dependence of the model parameters can be determined satisfactorily if we fit the model parameters one by one by applying a quadratic polynomial as a function of $\ln(s/s_0)$,

$$P(s) = p_0 + p_1 \ln(s/s_0) + p_2 \ln^2(s/s_0), \quad P \in \{R_q, R_d, R_{qd}, \alpha\}, \quad (11)$$

where p_0, p_1, p_2 are free parameters and s_0 is fixed on 1 GeV^2 . The results are shown in Fig. 23.

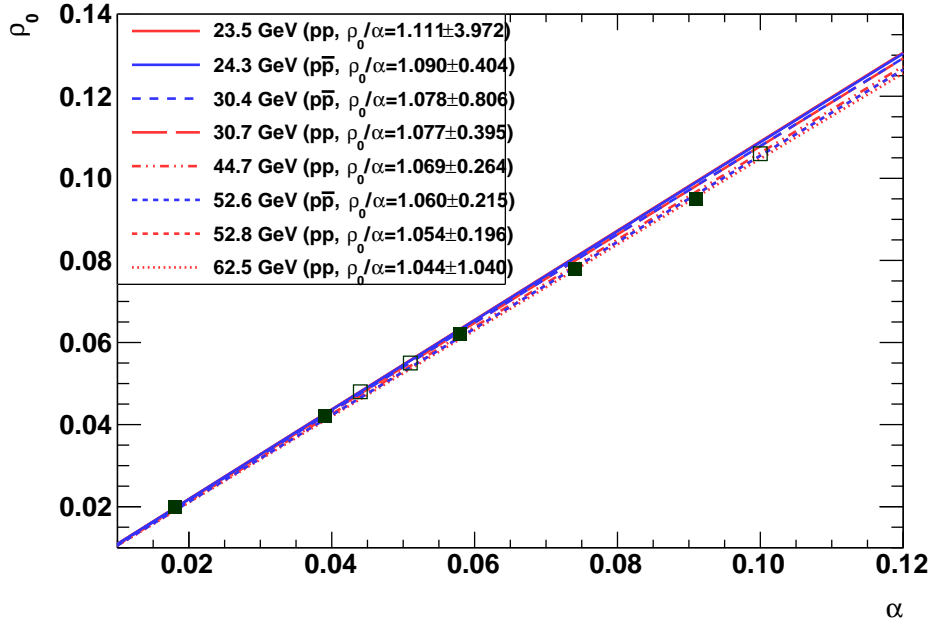


FIG. 21. Linearity between the ρ_0 -parameter and the α parameter of the ReBB model in the few tens of GeV energy region calculated from the trends of the scale parameters, $R_q(s)$, $R_d(s)$, $R_{qd}(s)$, corresponding to Figs. 23a-23c. The square shaped markers in the figure are positioned to the experimentally measured ρ_0 parameter values. In the ISR energy range, the ratio $\rho_0(s)/\alpha(s)$ is in an excellent agreement with the analytic approximations given by eq. (A11) of A, as also illustrated on Fig. 22.

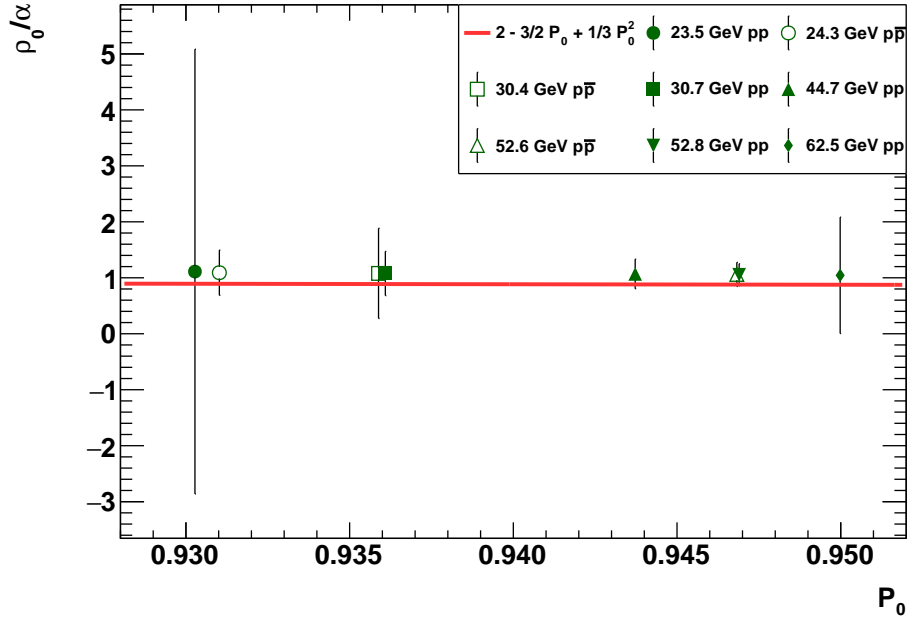


FIG. 22. The dependence of ρ_0/α on P_0 in the few tens of GeV energy range. Filled and empty symbols correspond to the pp and $p\bar{p}$ cases, respectively. These values and the error-bars for $\alpha(s)$ are obtained from the ReBB model fits to these datasets, by using the the excitation functions of the scale parameters $R_q(s)$, $R_d(s)$, $R_{qd}(s)$, shown in Figs. 23a-23c, and summarized in Table II. Where available, the experimentally measured ρ -parameter values were used for a comparison. The red curve represents the analytic result, corresponding to eq. (A11) in A, showing a good agreement between the analytic considerations and the numerical results.

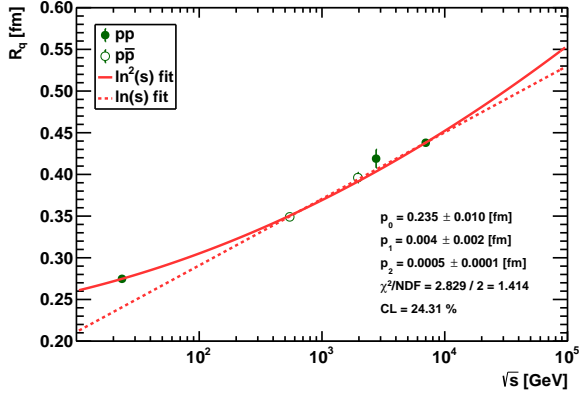
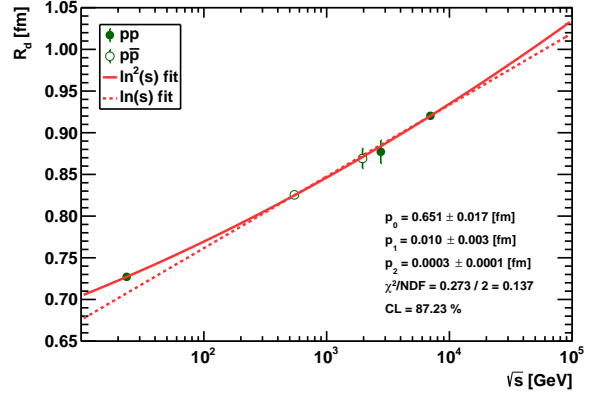
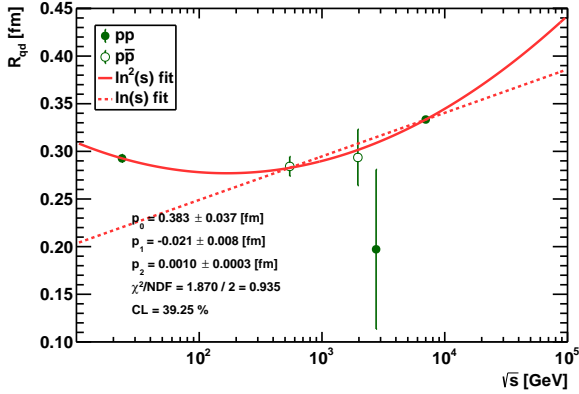
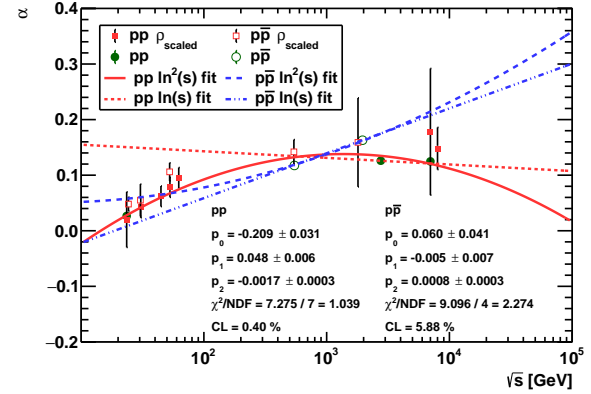
(a) Parameter R_q (b) Parameter R_d (c) Parameter R_{qd} (d) Parameter α

FIG. 23. The energy dependence of the parameters of the ReBB model, R_q , R_d , R_{qd} and α , taken from Fig. 20 and Table I, determined by fitting a second order logarithmic polynomial, Eq. (11), to each of them one by one in the energy range of $23.5 \leq \sqrt{s} \leq 8000$ GeV. As a comparison these figures also show the result of the fit in the energy range of $546 \leq \sqrt{s} \leq 8000$ GeV with the linear logarithmic model determined by the parameters collected in Table II. It is clear that allowing for quadratic corrections does not change significantly the linear trends in the kinematic range of $0.5 \leq \sqrt{s} \leq 8$ TeV.

We have performed several cross-checks to test the reliability of our fit at $\sqrt{s} = 7$ TeV. One of these related to the handling of the asymmetric type B t-dependent systematic errors. We have performed cross-checks for taking at every point either the smaller or the larger of the up and down type B errors to have a lower or an upper limit on their effects. We found that the parameters of the ReBB model remained stable for such a symmetrization

of the type B systematic errors, as the modification of the fit parameters due to such a symmetrization was within the quoted errors on the fit parameters. So we conclude that the fit is stable for small symmetrization of the type B systematic errors.

We see that the ReBB model has a leading order exponential feature. If we want to describe the significantly non-exponential features of differential cross-section in the low $|t|$ range [7, 59], the model has to be generalized for a possible non-exponential behaviour at low $|t|$. We plan to present such a generalization subsequently.

Let us also discuss the limitations of our method. The very precisely measured, pp TOTEM data at $\sqrt{s} = 13$ TeV data can not be described by the ReBB model in a statistically acceptable manner, so this model needs to be generalized further to describe the new features apparent in this dataset. These new features include the statistically significant non-exponential behaviours at low $-t$ observed both at 8 and 13 TeV in refs. [7, 59], the hollowness effect discussed in refs. [30, 73–75], the increased nuclear slope $B(s)$ and the increased ratio of the elastic to total cross-section discussed in ref. [61].

IX. SUMMARY

Currently, the statistically significant observation of the elusive Odderon is a hot research topic, with several interesting and important results and contributions. In the context of this manuscript, Odderon exchange corresponds to a crossing-odd component of the scattering amplitude of elastic proton-proton and proton-antiproton collisions, that does not vanish at asymptotically high energies, as probed experimentally by the D0 Collaboration for proton-antiproton and by the TOTEM Collaboration for proton-proton elastic collisions in the TeV energy range. Theoretically, the observed differences can be attributed only to the effect of a C-odd exchange, as detailed recently in refs. [30–32]. Those model independent studies resulted in an at least 6.26σ statistical significance of the Odderon exchange [30–32]. The goal of the research summarized in this manuscript was to cross-check, in a model-dependent way, the persistence of these Odderon-effects, and to provide a physical picture to interpret these results.

Using the ReBB model of ref. [36], developed originally to describe precisely the differential cross-section of elastic proton-proton collisions, we were able to describe also the proton-antiproton differential cross section at $\sqrt{s} = 0.546$ and 1.96 TeV without any modification of formalism. We have shown also that this model describes the proton-proton differential cross section at $\sqrt{s} = 2.76$ and 7 TeV, also in a statistically acceptable manner, with a CL > 0.1 %.

Using our good quality, statistically acceptable fits for the $\sqrt{s} \leq 8$ TeV, we have determined the energy dependence of the model parameters to be an affine linear function of $\ln(s/s_0)$. We have verified this energy dependence by demonstrating that the excitation functions of the physical parameters of the Real Extended Bialas-Bzdak model satisfy the so-called sanity tests: they describe in a statistically acceptable manner not only those four datasets that formed the basis of the determination of the excitation function, but all other published datasets in the $\sqrt{s} = 0.541 - 8.0$ TeV energy domain. We have also demonstrated that the excitation functions for the total cross-sections and the real-to-imaginary part ratios correspond to the experimentally established trends. Subsequently, we have also predicted the details of the diffractive interference (dip and bump) region at $\sqrt{s} = 0.9, 4, 5$ and 8 TeV. Currently, TOTEM preliminary experimental data are publicly presented from an on-going analysis at $\sqrt{s} = 8$ TeV, see ref. [58] for further details.

Remarkably, we have observed that the energy dependence of the geometrical scale parameters for pp and $p\bar{p}$ scattering are identical in elastic proton-proton and proton-antiproton collisions: only the energy dependence of the shape or opacity parameter $\alpha(s)$ differs significantly between pp and $p\bar{p}$ collisions. After determining the energy dependence of the model parameters we made extrapolations in order to compare the pp and $p\bar{p}$ differential cross sections in the few TeV energy range, corresponding to the energy of D0 measurement at $\sqrt{s} = 1.96$ TeV in ref. [53] and the TOTEM measurements at $\sqrt{s} = 2.76$ and 7.0 TeV. Doing this, we found evidence for the Odderon exchange with a high statistical significance. We have cross-checked, that this evidence withstands several reasonable cross-checks, for example the possible presence of small quadratic terms of $\ln(s/s_0)$ in the excitation functions of the parameters of this model.

We have shown that within the framework of this ReBB model, the very different trend of $\rho(s)$ in proton-proton and in proton-antiproton collisions enhances the model-independent Odderon signal, from a 6.26σ and 6.55σ effect of refs. [30–32] to an at least 7.1σ effect, obtained by the comparison of the differential cross-section of elastic proton-antiproton collisions to the currently lowest TOTEM energies of $\sqrt{s} = 2.76$ TeV. This significance increases to an even larger significance of an Odderon observation, when we extrapolate the differential cross-section of elastic proton-antiproton collisions to $\sqrt{s} = 7.0$ TeV. Given that a 7.1σ effect is already well above the usual 5σ , statistically significant discovery level, we are satisfied with the statistical significance level of our results at $\sqrt{s} = 2.76$ TeV, and quote it as the possibly lowest level of the significance of our model-dependent Odderon observation. Let us also emphasize that our Odderon observation is valid in the limited kinematic range of $0.541 \leq \sqrt{s} \leq 8$ TeV center of mass energy and in the $0.377 \leq -t \leq 1.2$ GeV² four-momentum transfer range.

Concerning the direction of future research: Odderon is now discovered both in a model-independent way, described in refs. [30–32], and in a model-dependent way, described in this manuscript. So the obvious next step is to extract its detailed properties, both in a model-independent and in a model-dependent manner.

Let us also note, that the ReBB model as presented in ref. [36] does not yet provide a statistically acceptable fit quality to the differential cross-section of $\sqrt{s} = 13$ TeV elastic pp scattering. This might be due to the emergence of the black-ring limit of elastic proton-proton scattering instead of the expected black-disc limit, as detailed in ref. [61], or due to

the very strong non-exponential features of the differential cross-sections in these collisions at low $-t$, as shown in ref. [6, 7]. So we conclude that the Real Extended Bialas-Bzdak model needs to be further generalized for the top LHC energies and above. This work is in progress, but it goes clearly well beyond the scope of the current, already rather detailed manuscript. Importantly, any possible outcome of these follow-up studies is not expected to modify the model behavior at the presently investigated energy range, and hence it is not necessary to the task solved in this manuscript.

In short, we determined the model-dependent statistical significance of the Odderon observation to be an at least 7.1σ effect in the $0.5 \leq \sqrt{s} \leq 8$ TeV center of mass energy and $0.377 \leq -t \leq 1.2$ GeV² four-momentum transfer range. Our analysis is based on the analysis of published D0 and TOTEM data of refs. [6, 9, 53] and uses as a tool the Real Extended Bialas-Bzdak model of ref. [36]. We have cross-checked that this unitary model works in a statistically acceptable, carefully tested and verified manner in this particular kinematic range. Our main results are illustrated on Figs. 17 and 18.

ACKNOWLEDGMENTS

First of all, we would like to thank F. Nemes, who initiated this project, and started to test the Real Extended Bialas-Bzdak model against the proton-antiproton data. He also provided several valuable technical help for us in the initial phases of these studies.

We gratefully acknowledge inspiring discussions with C. Avila, S. Giani, P. Grannis, G. Gustafson, L. Jenkovszky, E. Levin, T. Novák, K. Österberg, R. Pasechnik, C. Royon, A. Ster and M. Strikman. Our research has been partially supported by the ÚNKP-18-2 New National Excellence Program of the Ministry of Human Capacities, and by the NKFIH grants No. FK-123842, FK-123959 and K133046 as well as by the EFOP 3.6.1-16-2016-00001 grant (Hungary), as well as by the framework of the COST Action CA15213 “Theory of hot matter and relativistic heavy-ion collisions (THOR)” of the European Union.

Appendix A: On the proportionality between $\rho_0(s)$ and $\alpha(s)$

Let us first of all note that the detailed description of the Real Extended Bialas-Bzdak (ReBB) model is given in Section 2.2 of ref. [36]. We have utilized that formalism throughout the fits described in the body of the manuscript, however in this Appendix, we need to develop this formalism a bit further, as in the earlier publications the details of the relations between the ρ parameter (the ratio of the real to the imaginary part of the scattering amplitude at $t = 0$) and the parameter α of the ReBB model (that is responsible for filling up the singular dip of the original Bialas-Bzdak model of refs. [37–40]) has not yet been detailed before.

First of all, let us note that ReBB model is unitary, by definition. Thus the elastic scattering amplitude in the ReBB model too has the following unitary form

$$t_{el}(s, b) = i \left(1 - e^{-\Omega(s, b)} \right), \quad (\text{A1})$$

where the opacity function $\Omega(s, b)$ is, in general, a complex valued function. The shadow profile function is given as

$$P(s, b) = 1 - |\exp(-\Omega)|^2 = \tilde{\sigma}_{inel}(s, b), \quad (\text{A2})$$

and this is the reason why the shadow profile function is also frequently called as the inelastic profile function, as it describes the probability distribution of inelastic collisions in the impact parameter space. This inelastic profile function was evaluated with the help of Glauber's multiple diffraction theory [42] for the colliding protons consisting a constituent quark and diquark or $p = (q, d)$ picture in Section 2.2 of ref. [36] and the results were visualized in Figs. 5 and 9 of that paper. These were also evaluated precisely and in a model-independent way, using the Levy series method, in ref. [76], where the error band around the shadow profiles has also been determined and it was shown that at lower energies, these shadow profiles have a maximum in their center, while at $\sqrt{s} = 13$ TeV, a small but statistically significant hollow develops inside the protons, as originally proposed in refs. [73–75].

In the Bialas-Bzdak model, the imaginary part of $\Omega(s, b)$, that determines the real part of the scattering amplitude, was assumed to be negligibly small in the first publications of refs. [37–40]. However, eq. (29) of ref. [36] introduced this, generally unknown, imaginary part of

the complex opacity function $\Omega(s, b)$ so that it is proportional to the probability of inelastic scatterings, $\tilde{\sigma}_{inel}(s, b)$, which are typically decreasing functions of the impact parameter b . A possible interpretation of this assumption may be that the inelastic collisions arise from non-collinear elastic collisions of the constituent of protons, the quarks and diquarks, hence the elastic collisions follow the same spatial distributions as the inelastic collisions of the same constituents:

$$\text{Im } \Omega(s, b) = -\alpha \tilde{\sigma}_{inel}(s, b). \quad (\text{A3})$$

The above definition of eq. (A3) subsequently leads to the following expression for the impact parameter dependence of the scattering amplitude:

$$t_{el}(s, b) = i \left(1 - e^{i\alpha \tilde{\sigma}_{in}(s, b)} \sqrt{1 - \tilde{\sigma}_{in}(s, b)} \right). \quad (\text{A4})$$

This result is obtained using only unitarity and the ansatz of eq. (A3), but without any further approximations. From now on, we develop two small set of approximations that are based on the physical domain of the ReBB model parameters.

From the fits performed so far, we always find $\alpha \lesssim 0.165$, corresponding to Table 1 of ref. [36] and Table I of the current manuscript.

In these physical cases, when $\alpha \tilde{\sigma}_{in}(s, b) \ll 1$ is small, one obtains for the real and imaginary parts, respectively,

$$\text{Re } t_{el}(s, b) = \alpha \tilde{\sigma}_{in}(s, b) \sqrt{1 - \tilde{\sigma}_{in}(s, b)} \quad (\text{A5})$$

and

$$\text{Im } t_{el}(s, b) = 1 - \sqrt{1 - \tilde{\sigma}_{in}(s, b)}. \quad (\text{A6})$$

Given that the real part of the scattering amplitude is thus proportional to α while the imaginary part is independent of α , we indeed find that

$$\rho \propto \alpha, \quad \text{if } \alpha \ll 1. \quad (\text{A7})$$

Based on Figs. 5 and 9. of ref. [36] and the model-independent results of the Levy series method detailed in ref. [76], if the colliding energy is in the $\sqrt{s} \leq 8$ TeV domain, corresponding to the domain of our extrapolations, the shadow profile function is nearly

Gaussian. Such a behaviour can be obtained easily as follows:

Let us approximate the imaginary part of the scattering amplitude with a Gaussian, *i.e.*,

$$\text{Im } t_{el}(s, b) \simeq \lambda(s) \exp\left(-\frac{b^2}{2R(s)}\right). \quad (\text{A8})$$

Then the inelastic profile or shadow profile function takes the form of

$$\tilde{\sigma}_{in}(s, b) = 2\lambda(s) \exp\left(-\frac{b^2}{2R(s)}\right) - \lambda(s)^2 \exp\left(-\frac{b^2}{R(s)^2}\right). \quad (\text{A9})$$

This expression, up to second order terms, starts as a Gaussian, but it actually corresponds to the subtraction of a broader and smaller Gaussian from a narrower and larger Gaussian in the physical domain of $\lambda(s) \leq 1$.

As $P_0 \equiv P(s, 0) = \tilde{\sigma}_{inel}(s, b = 0)$ is the value of the shadow profile or inelastic profile function at $b = 0$, we find the following relation between P_0 and $\lambda(s)$:

$$P_0(s) = 2\lambda(s) - \lambda^2(s) \leq 1. \quad (\text{A10})$$

When performing the transformation from the impact parameter space to momentum space, the result for the real to imaginary part ratio of the forward scattering amplitude, defined by Eq. (5), is

$$\rho(s) = \alpha(s) \left(2 - \frac{3}{2}P_0(s) + \frac{1}{3}P_0^2(s)\right). \quad (\text{A11})$$

Based on the formalism of Section 2.2 of ref. [36], $P_0 \equiv P_0(s)$ is a function of $R_q(s)$, $R_d(s)$ and $R_{qd}(s)$ only, but otherwise it is independent of the fourth physical parameter of the Real Extended Bialas-Bzdak model, $\alpha(s)$. Hence the excitation function of $P_0(s)$ is determined completely by the parameters p_1 and p_0 of the excitation functions of the scale parameters (R_q, R_d, R_{qd}) , as summarized in Table II. This way, the $P_0 = P_0(R_q(s), R_d(s), R_{qd}(s))$ function is uniquely given by with the help of eq. (A3), corresponding to eq. (29) of ref. [36].

We have cross-checked the result of these analytic considerations compared to the fit results on $\alpha(s)$ and the measured values of $\rho_0(s)$ at the ISR energies and we find an excellent agreement between the analytic approximations and the numerical results at ISR, corresponding to the $P_0(s)$ range of 0.93 - 0.95, as illustrated on Fig. 22. The linear rela-

tionship between ρ_0 and the ReBB model parameter α is also indicated at the ISR energy range, on Fig. 21. Similarly, we find an excellent agreement between the analytic calculations of eq. (A11) and the numerical and experimental results at the few TeV energy scale of $0.5 \leq \sqrt{s} \leq 8$ TeV, as demonstrated on Fig. 7, presented in the body of this manuscript.

-
- [1] L. Lukaszuk and B. Nicolescu, *Lett. Nuovo Cim.* **8**, 405 (1973), doi:10.1007/BF02824484.
- [2] J. Bartels, L. Lipatov and G. Vacca, *Phys. Lett. B* **477**, 178 (2000), arXiv:hep-ph/9912423, doi:10.1016/S0370-2693(00)00221-5.
- [3] L. L. Jenkovszky, A. I. Lengyel and D. I. Lontkovskyi, *Int. J. Mod. Phys. A* **26**, 4755 (2011), arXiv:1105.1202 [hep-ph], doi:10.1142/S0217751X11054760.
- [4] A. Ster, L. Jenkovszky and T. Csörgő, *Phys. Rev.* **D91**, 074018 (2015), arXiv:1501.03860 [hep-ph], doi:10.1103/PhysRevD.91.074018.
- [5] A. Breakstone *et al.*, *Phys. Rev. Lett.* **54**, 2180 (1985), doi:10.1103/PhysRevLett.54.2180.
- [6] TOTEM Collaboration (G. Antchev *et al.*), *Eur. Phys. J.* **C79**, 103 (2019), arXiv:1712.06153 [hep-ex], doi:10.1140/epjc/s10052-019-6567-0.
- [7] TOTEM Collaboration (G. Antchev *et al.*) (2017), arXiv:1812.04732 [hep-ex].
- [8] TOTEM Collaboration (G. Antchev *et al.*) (2018), arXiv:1812.08283 [hep-ex].
- [9] TOTEM Collaboration (G. Antchev *et al.*) (2018), arXiv:1812.08610 [hep-ex].
- [10] V. A. Khoze, A. D. Martin and M. G. Ryskin, *Phys. Rev.* **D97**, 034019 (2018), arXiv:1712.00325 [hep-ph], doi:10.1103/PhysRevD.97.034019.
- [11] A. P. Samokhin and V. A. Petrov, *Nucl. Phys.* **A974**, 45 (2018), arXiv:1708.02879 [hep-ph], doi:10.1016/j.nuclphysa.2018.03.009.
- [12] T. Csörgő, R. Pasechnik and A. Ster, *Eur. Phys. J.* **C79**, 62 (2019), arXiv:1807.02897 [hep-ph], doi:10.1140/epjc/s10052-019-6588-8.
- [13] M. Broilo, E. G. S. Luna and M. J. Menon, *Phys. Rev.* **D98**, 074006 (2018), arXiv:1807.10337 [hep-ph], doi:10.1103/PhysRevD.98.074006.
- [14] G. Pancheri, S. Pacetti and Y. Srivastava, *Phys. Rev.* **D99**, 034014 (2019), arXiv:1811.00499 [hep-ph], doi:10.1103/PhysRevD.99.034014.
- [15] V. P. Goncalves and P. V. R. G. Silva, *Eur. Phys. J.* **C79**, 237 (2019), arXiv:1811.12250 [hep-ph], doi:10.1140/epjc/s10052-019-6768-6.
- [16] O. Selyugin and J. Cudell, *Acta Phys. Polon. Supp.* **12**, 741 (2019), arXiv:1810.11538 [hep-ph], doi:10.5506/APhysPolBSupp.12.741.
- [17] V. A. Khoze, A. D. Martin and M. G. Ryskin, *Phys. Lett.* **B780**, 352 (2018), arXiv:1801.07065 [hep-ph], doi:10.1016/j.physletb.2018.03.025.

- [18] M. Broilo, E. G. S. Luna and M. J. Menon, *Phys. Lett.* **B781**, 616 (2018), [arXiv:1803.07167](#) [hep-ph], doi:10.1016/j.physletb.2018.04.045.
- [19] S. M. Troshin and N. E. Tyurin, *Mod. Phys. Lett.* **A33**, 1850206 (2018), [arXiv:1805.05161](#) [hep-ph], doi:10.1142/S0217732318502061.
- [20] I. M. Dremin, *Universe* **4**, 65 (2018), doi:10.3390/universe4050065.
- [21] E. Martynov and B. Nicolescu, *Phys. Lett.* **B786**, 207 (2018), [arXiv:1804.10139](#) [hep-ph], doi:10.1016/j.physletb.2018.09.049.
- [22] E. Martynov and B. Nicolescu, *Eur. Phys. J. C* **79**, 461 (2019), [arXiv:1808.08580](#) [hep-ph], doi:10.1140/epjc/s10052-019-6954-6.
- [23] Y. M. Shabelski and A. G. Shuvaev, *Eur. Phys. J.* **C78**, 497 (2018), [arXiv:1802.02812](#) [hep-ph], doi:10.1140/epjc/s10052-018-5979-6.
- [24] V. A. Khoze, A. D. Martin and M. G. Ryskin, *Phys. Lett.* **B784**, 192 (2018), [arXiv:1806.05970](#) [hep-ph], doi:10.1016/j.physletb.2018.07.054.
- [25] Y. Hagiwara, Y. Hatta, R. Pasechnik and J. Zhou (2020), [arXiv:2003.03680](#) [hep-ph].
- [26] C. Contreras, E. Levin, R. Meneses and M. Sanhueza (2020), [arXiv:2004.04445](#) [hep-ph].
- [27] E. Gotsman, E. Levin and I. Potashnikova (2020), [arXiv:2003.09155](#) [hep-ph].
- [28] E. Gotsman, E. Levin and I. Potashnikova, *Phys. Lett.* **B786**, 472 (2018), [arXiv:1807.06459](#) [hep-ph], doi:10.1016/j.physletb.2018.10.017.
- [29] V. A. Petrov and A. P. Samokhin, *Int. J. Mod. Phys. Conf. Ser.* **47**, 1860097 (2018), [arXiv:1801.03809](#) [hep-ph], doi:10.1142/S2010194518600972.
- [30] T. Csörgő, T. Novák, R. Pasechnik, A. Ster and I. Szanyi (12 2019), [arXiv:1912.11968](#) [hep-ph].
- [31] T. Csörgő, T. Novák, R. Pasechnik, A. Ster and I. Szanyi, Proton Holography – Discovering Odderon from Scaling Properties of Elastic Scattering, in *49th International Symposium on Multiparticle Dynamics*, (4 2020). [arXiv:2004.07095](#) [hep-ph].
- [32] T. Csörgő, T. Novák, R. Pasechnik, A. Ster and I. Szanyi (4 2020), [arXiv:2004.07318](#) [hep-ph].
- [33] F. Nemes and T. Csörgő, *Int. J. Mod. Phys. A* **27**, 1250175 (2012), [arXiv:1204.5617](#) [hep-ph], doi:10.1142/S0217751X12501758.
- [34] T. Csörgő and F. Nemes, *Int. J. Mod. Phys. A* **29**, 1450019 (2014), [arXiv:1306.4217](#) [hep-ph], doi:10.1142/S0217751X14500195.

- [35] T. Csörgő, R. Glauber and F. Nemes, Elastic proton-proton scattering from ISR to LHC energies, focusing on the dip region, in *International Workshop on Low X Physics*, (11 2013). [arXiv:1311.2308 \[hep-ph\]](#).
- [36] F. Nemes, T. Csörgő and M. Csanád, *Int. J. Mod. Phys. A* **30**, 1550076 (2015), [arXiv:1505.01415 \[hep-ph\]](#), doi:10.1142/S0217751X15500761.
- [37] A. Bialas and A. Bzdak, *Phys. Lett. B* **649**, 263 (2007), [arXiv:nucl-th/0611021](#), doi:10.1016/j.physletb.2007.04.014, [Erratum: *Phys.Lett.B* 773, 681–681 (2017)].
- [38] A. Bzdak, *Acta Phys. Polon. B* **38**, 2665 (2007), [arXiv:hep-ph/0701028](#).
- [39] A. Bialas and A. Bzdak, *Acta Phys. Polon. B* **38**, 159 (2007), [arXiv:hep-ph/0612038](#).
- [40] A. Bialas and A. Bzdak, *Phys. Rev. C* **77**, 034908 (2008), [arXiv:0707.3720 \[hep-ph\]](#), doi:10.1103/PhysRevC.77.034908.
- [41] R. Glauber, *Phys. Rev.* **100**, 242 (1955), doi:10.1103/PhysRev.100.242.
- [42] R. Glauber and G. Matthiae, *Nucl. Phys. B* **21**, 135 (1970), doi:10.1016/0550-3213(70)90511-0.
- [43] R. J. Glauber, *Nucl. Phys. A* **774**, 3 (2006), [arXiv:nucl-th/0604021](#), doi:10.1016/j.nuclphysa.2006.06.009.
- [44] W. Czyz and L. Maximon, *Annals Phys.* **52**, 59 (1969), doi:10.1016/0003-4916(69)90321-2.
- [45] T. Regge, *Nuovo Cim.* **14**, 951 (1959), doi:10.1007/BF02728177.
- [46] P. D. B. Collins, *An Introduction to Regge Theory and High-Energy Physics* Cambridge Monographs on Mathematical Physics, Cambridge Monographs on Mathematical Physics (Cambridge Univ. Press, Cambridge, UK, 2009).
- [47] L. Jenkovszky, R. Schicker and I. Szanyi, *Int. J. Mod. Phys. E* **27**, 1830005 (2018), [arXiv:1902.05614 \[hep-ph\]](#), doi:10.1142/S0218301318300059.
- [48] A. Donnachie and P. Landshoff, *Nucl. Phys. B* **231**, 189 (1984), doi:10.1016/0550-3213(84)90283-9.
- [49] PHENIX Collaboration (A. Adare *et al.*), *Phys. Rev.* **C77**, 064907 (2008), [arXiv:0801.1665 \[nucl-ex\]](#), doi:10.1103/PhysRevC.77.064907.
- [50] TOTEM Collaboration (G. Antchev *et al.*), *EPL* **101**, 21002 (2013), doi:10.1209/0295-5075/101/21002.
- [51] UA4 Collaboration (R. Battiston *et al.*), *Phys. Lett.* **127B**, 472 (1983), doi:10.1016/0370-2693(83)90296-4.
- [52] UA4 Collaboration (M. Bozzo *et al.*), *Phys. Lett.* **155B**, 197 (1985), doi:10.1016/0370-

- 2693(85)90985-2.
- [53] D0 Collaboration (V. M. Abazov *et al.*), *Phys. Rev.* **D86**, 012009 (2012), [arXiv:1206.0687 \[hep-ex\]](#), doi:10.1103/PhysRevD.86.012009.
- [54] Particle Data Group Collaboration (M. Tanabashi *et al.*), *Phys. Rev. D* **98**, 030001 (2018), doi:10.1103/PhysRevD.98.030001.
- [55] COMPETE Collaboration (J. R. Cudell, V. V. Ezhela, P. Gauron, K. Kang, Yu. V. Kuyanov, S. B. Lugovsky, E. Martynov, B. Nicolescu, E. A. Razuvaev and N. P. Tkachenko), *Phys. Rev. Lett.* **89**, 201801 (2002), [arXiv:hep-ph/0206172 \[hep-ph\]](#), doi:10.1103/PhysRevLett.89.201801.
- [56] F. J. Nemes, *PoS DIS2017*, 059 (2018), doi:10.22323/1.297.0059.
- [57] TOTEM Collaboration (G. Antchev *et al.*), *EPL* **101**, 21003 (2013), doi:10.1209/0295-5075/101/21003.
- [58] J. Kaspar, *EPJ Web of Conferences* **172**, 06005 (2018), doi:10.1051/epjconf/201817206005.
- [59] TOTEM Collaboration (G. Antchev *et al.*), *Nucl. Phys.* **B899**, 527 (2015), [arXiv:1503.08111 \[hep-ex\]](#), doi:10.1016/j.nuclphysb.2015.08.010.
- [60] TOTEM Collaboration (G. Antchev *et al.*), *Eur. Phys. J.* **C76**, 661 (2016), [arXiv:1610.00603 \[nucl-ex\]](#), doi:10.1140/epjc/s10052-016-4399-8.
- [61] TOTEM Collaboration, T. Csörgő, Recent Results from the CERN LHC Experiment TOTEM – Implications for Odderon Exchange, in *48th International Symposium on Multiparticle Dynamics (ISMD 2018) Singapore, Singapore, September 3-7, 2018*, (2019). [arXiv:1903.06992 \[hep-ex\]](#).
- [62] UA4/2 Collaboration (C. Augier *et al.*), *Phys. Lett. B* **316**, 448 (1993), doi:10.1016/0370-2693(93)90350-Q.
- [63] E710 Collaboration (N. A. Amos *et al.*), *Phys. Rev. Lett.* **68**, 2433 (1992), doi:10.1103/PhysRevLett.68.2433.
- [64] E-811 Collaboration (C. Avila *et al.*), *Phys. Lett. B* **537**, 41 (2002), doi:10.1016/S0370-2693(02)01908-1.
- [65] TOTEM Collaboration (G. Antchev *et al.*), *EPL* **101**, 21004 (2013), doi:10.1209/0295-5075/101/21004.
- [66] UA4 Collaboration (D. Bernard *et al.*), *Phys. Lett.* **B171**, 142 (1986), doi:10.1016/0370-2693(86)91014-2.

- [67] E-710 Collaboration (N. A. Amos *et al.*), *Phys. Lett. B* **247**, 127 (1990), doi:10.1016/0370-2693(90)91060-O.
- [68] TOTEM Collaboration (G. Antchev *et al.*), *Phys. Rev. Lett.* **111**, 012001 (2013), doi:10.1103/PhysRevLett.111.012001.
- [69] I. Szanyi, N. Bence and L. Jenkovszky, *J. Phys.* **G46**, 055002 (2019), arXiv:1808.03588 [hep-ph], doi:10.1088/1361-6471/ab1205.
- [70] A. Donnachie and P. Landshoff, *Nucl. Phys. B* **348**, 297 (1991), doi:10.1016/0550-3213(91)90520-8.
- [71] E. Nagy *et al.*, *Nucl. Phys. B* **150**, 221 (1979), doi:10.1016/0550-3213(79)90301-8.
- [72] U. Amaldi and K. R. Schubert, *Nucl. Phys.* **B166**, 301 (1980), doi:10.1016/0550-3213(80)90229-1.
- [73] W. Broniowski and E. Ruiz Arriola, *Acta Phys. Polon. B* **48**, 927 (2017), arXiv:1704.03271 [hep-ph], doi:10.5506/APhysPolB.48.927.
- [74] W. Broniowski and E. Ruiz Arriola, *Acta Phys. Polon. Supp.* **10**, 1203 (2017), arXiv:1708.00402 [nucl-th], doi:10.5506/APhysPolBSupp.10.1203.
- [75] W. Broniowski, L. Jenkovszky, E. Ruiz Arriola and I. Szanyi, *Phys. Rev. D* **98**, 074012 (2018), arXiv:1806.04756 [hep-ph], doi:10.1103/PhysRevD.98.074012.
- [76] T. Csörgő, R. Pasechnik and A. Ster, *Eur. Phys. J.* **C80**, 126 (2020), arXiv:1910.08817 [hep-ph], doi:10.1140/epjc/s10052-020-7681-8.